Scientific Research Publishing

Atmospheric and Climate Sciences, 2025, 15(1), 218-247
https://www.scirp.org/journal/acs
ISSN Online: 2160-0422
ISSN Print: 2160-0414

Intraseasonal Variability of Rainfall over Tanzania during March-April-May (MAM) Season of 2022

Chabaga Masoud Chabaga[1,2*], Godfrey Asenga[1,2], Daudi Ndabagenga[1,2]

[1]Key Laboratory of Meteorological Disasters of Ministry of Education, Collaborative Innovation Center on Forecast and Evaluation of Meteorological Disasters, Nanjing University of Information Science and Technology, Nanjing, China
[2]Tanzania Meteorological Authority, Dodoma, Tanzania
Email: *chabbys1983@gmail.com, met@meteo.go.tz

How to cite this paper: Chabaga, C.M., Asenga, G. and Ndabagenga, D. (2025) Intraseasonal Variability of Rainfall over Tanzania during March-April-May (MAM) Season of 2022. *Atmospheric and Climate Sciences*, **15**, 218-247.
https://doi.org/10.4236/acs.2025.151011

Received: November 27, 2024
Accepted: January 17, 2025
Published: January 20, 2025

Abstract

This study investigates the intraseasonal variability (ISV) of rainfall in Tanzania during the March-April-May (MAM) season, specifically identifying the dominant peaks of ISV in rainfall for that period. The 5-day running mean during the MAM season reveals that Tanzania experienced an irregular pattern of wet and dry days in the year 2022, indicating the presence of ISV that led to fluctuations in weather patterns. Moreover, the study identifies the dominant peak date, where a significant peak was observed in the 10 - 25-day range, showing that ISV exhibits a quasi-biweekly oscillation around 17 days, with composite evolution from day −8 to day +8 after filtering, and day 0 marking peak rainfall. Furthermore, composite atmospheric circulation analysis reveals critical interactions with ISV. Geopotential height wind patterns at 850 hPa indicate that negative/positive geopotential height anomalies over the Western Indian Ocean and Mozambique Channel enhance low-level convergence/divergence of moisture, resulting in wet/dry phase, meanwhile strong positive geopotential height anomalies at 200 hPa are associated with the upper-level divergence that supports peak rainfall (day 0). During Lag −4 to Lag 0, the results revealed dominant negative OLR anomalies (−18 to −20 W/m^2) indicating peak dates of ISV of rainfall while the transition to positive OLR anomalies after Lag +2 showed the starting point of a dry phase of ISV. Also, at the initial phase (Lag −8 to Lag −6), weak positive and limited moisture flux anomalies were observed over the region, while in the peak phase (Lag 0), strong positive anomalies dominated, reflecting intense moisture convergence from both the South West Indian Ocean (SWIO) and the Congo Basin, associated with maximum ISV of rainfall activity. After lag 0, transition into the dry phase (Lag +6 to Lag +8), negative anomalies developed as

moisture transport diminishes and winds shift, suppressing convergence over Tanzania, leading to the dry phase. The results highlight the significance of integrating ISV patterns into weather forecasting and disaster preparedness to reduce the risks associated with extreme rainfall events like floods and droughts. Additionally, the findings offer valuable insights for managing water resources, planning agriculture, and enhancing climate resilience in areas of Tanzania that depend on rainfall.

Keywords

Tanzania, Intraseasonal Variability, Rainfall, MAM, Atmospheric Circulation

1. Introduction

Like other countries in the world, Tanzania faces significant challenges associated with intraseasonal variability (ISV) of rainfall, specifically posing great impacts on rain-fed agriculture dependent communities [1] [2]. The ISV of rainfall in 2022 March, April and May (MAM) season in Tanzania was characterized by extreme weather events, with the northern coast and northeastern highlands experiencing severe drought, receiving less than 50% of the usual rainfall, making it the 15th driest year on record and the second driest MAM season since 1970, according to the Tanzania Meteorological Authority [3]. On the other hand, heavy rainfall in April 2022 caused severe flooding in Mbeya and Songwe regions, resulting in 5 deaths, 21 injuries, 5 missing persons, and 3150 displaced people, with significant damage to infrastructure, including 400 houses, 35 schools, as well as losses to agriculture and livestock, including 24,700 acres of farm fields and 2362 livestock. Also, according to [4] ISV of rainfall in Tanzania resulted in mudslides in the Hanang District of the Manyara Region causing rocks, logs, and a lot of water to pour from Mount Hanang towards Katesh Township. The report indicated that at least 72 fatalities occurred, 117 injuries, and 5600 affected individuals. In addition, 750 acres of various crops were damaged by the rain and water, and livestock were also lost. The environment, health and education services, and infrastructure such as roads, water sources, energy, and communication systems were all devastated. The above problems bring the necessity to investigate the ISV of rainfall in Tanzania for MAM 2022.

A number of studies about ISV in East Africa and Tanzania have been investigated. A study conducted by [5] indicated that the convection over western Tanzania is associated with moisture flux from the tropical southeast Atlantic and Congo Basin, followed by weak easterlies from the western Indian Ocean, which results in the intraseasonal variability of rainfall. Also, the research showed that ISV are vital in tropical regions, exhibiting distinct characteristics regarding their timing and propagation. The study of [6] explained that Indian Ocean Dipole plays a key role in determining rainfall patterns in East Africa, with significant

implications for both climate variability and socioeconomic stability in the region. According to [7], IOD explains about 12% of the variability in sea surface temperatures in the Indian Ocean and leads to intense rainfall variability in eastern Africa during its active phases. According to [8] Rainfall patterns in East Africa are also shaped by the interaction between subtropical high-pressure systems and moisture from the Congo Basin and the SWIO. The influence of the St. Helena High and the Azores High is particularly crucial for the region's climate during the MAM season [9]. When the St. Helena High intensifies, it facilitates increased moisture influx from the Congo Basin, while southeasterly winds from the Mascarene High enhance this moisture transport. This interaction promotes greater convection and significant rainfall, specifically in the northwestern and western regions near Lake Victoria [10]. Since [11] first applied spectral analysis to identify a 40 - 50-day eastward-propagating oscillation in the tropics, attention to the characteristics and mechanisms of intraseasonal oscillations (ISOs) has been increasing. The studies [12] identified significant intra-seasonal oscillations in convection over tropical East Africa during the December to February rainy season and revealed dominant cycles of 16 to 33 days, with active and passive convective phases frequent within the rainy season. Also, [13] found that the synoptic-scale forcing has critical role shaping intra-seasonal oscillations in driving rainfall variability over East Africa. According to [14] the study identified two key intraseasonal oscillatory modes with periods of about 45 days and 28 days align with the active and pause phases of monsoon rainfall over India, where the active phase is considered by enhanced convection, and the break phase is marked by dry weather conditions. The study of [15] indicates that primary intraseasonal rainfall variability during Rwanda's long rainy season (February-May) occurs on a 10 - 25-day time scale. The study indicates the importance of considering both ISO and MJO in understanding rainfall variability in Central Africa [16].

Despite different studies conducted to investigate the ISV, there has been limited research specifically focusing on this aspect in Tanzania. Most studies concentrated on inter-annual, inter-seasonal, and inter-decadal time scales [17]-[19]. Still there is no clear understanding of the dominant peak date for ISV of rainfall over Tanzania during the MAM season. Therefore, the aim of this research is to investigate the ISV of rainfall over Tanzania during MAM season of 2022 by employing power spectrum method. Furthermore, Atmospheric circulation is investigated to assess its relationship with ISV. Such findings are crucial for agricultural planning, enabling farmers to make well-informed decisions based on expected rainfall, and they also contribute to disaster risk management by training communities to prepare for possible flooding and other weather-related issues. The remainder of this paper is organized as follows: The data and methods employed are described in Section 2. In Section 3, the Results of dominant modes of the intraseasonal variability (ISV) of the rainfall variability in Tanzania are revealed. In Section 4, the atmospheric circulation influence to ISV. Finally, Discussion and Conclusion in Section 5.

2. Data and Methodology

2.1. Study Area

Tanzania, is located in East Africa through the longitudinal range of 28˚E to 42˚E and the latitudinal range of 12˚S to 0˚S (Figure 1). It has an estimated population of 62 million people spread across 947,300 square kilometers [20]. As one of Africa's most densely populated nations. The Country has large network of weather stations which poses both manual and automatic for particular focused on agricultural meteorology and synoptic station. Several factors signify influence of the distribution and variability of rainfall in Tanzania. Key contributors include the East African Monsoon, the El Niño Southern Oscillation (ENSO), westerlies from the Congo, tropical cyclones, and the Inter-Tropical Convergence Zone (ITCZ). The East African Monsoon is known to bring seasonal rains in East Africa [21] [22], while ENSO events lead to extensive oscillations in rainfall patterns

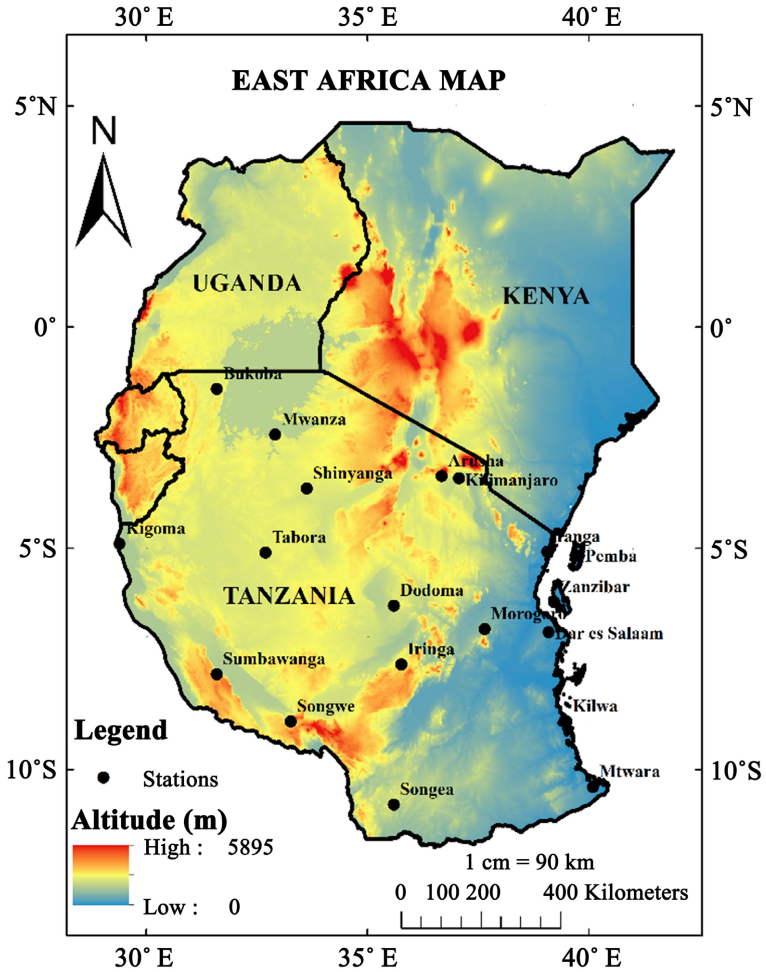

Figure 1. The study area (Tanzania), as shown on the map of East Africa, is bounded by latitude 0˚ - 12˚S and longitude 28˚ - 42˚E. The map highlights selected rainfall monitoring stations (black circles) used to analyze the intraseasonal variability (ISV) of rainfall during the MAM rainy season. Elevation is represented by a color gradient, with red indicating high altitudes (up to 5895 m) and blue representing low-lying areas.

[23], whereas La Niña tends to result in drier conditions [24]. Furthermore, the westerlies originating from the Congo contribute moisture to the western regions of the country, and tropical cyclones can irregularly impact coastal areas, bringing heavy rainfall [25]. The migration of ITCZ north and south across the equator are among the main factors affecting distribution and variability of rainfall in Tanzania and the entire East Africa [26]. The migration of ITCZ lags the overhead sun by 3 - 4 weeks over the region.

The ITCZ migrates to southern regions of Tanzania in October to December, reaching the southern part of the country in January-February and reverses northwards in March, April and May [3] [17]. Due to this movement, some areas experience single and double passages of the ITCZ. The areas that coincide with single passage are known as unimodal areas. These include the southern, southwestern, central, and western parts of the country, which receive rainfall from November to April or May (NDJFMA, also known as Msimu). Areas that experience double passage are known as bimodal, and include northern coast, northeastern highlands, Lake Victoria basin, and the Islands of Zanzibar (Unguja and Pemba). These regions receive two distinct rainfall seasons. The long rain season (also known as Masika), which starts mainly in March and continues through May (MAM) and the short rainfall season (also called Vuli) which starts in October and continues through December (OND). January and February are the transition period (relatively dry) for bimodal areas while June, July, August, and September are dry months for the entire country [3].

2.2. Data Source

2.2.1. Observation Data

To analyze ISV of rainfall, the study utilized daily rainfall observation data from 18 scattered synoptic stations (**Figure 1**) provided by the Tanzania Meteorological Authority (TMA) for the year 2022. The data are measured and collected daily at each station using a rain gauge.

2.2.2. Reanalyzed Data

Analysis of spatial climatology and time evolution of rainfall over the region utilized daily precipitation data (1981-2022) from CHIRPS (Climate Hazards Group Infrared Precipitation with Station) version 2.0 with worldwide coverage of 50˚S - 50˚N latitude and spatial resolution at 0.05˚ - 0.05˚ latitude-longitude grid from 1981 to present [27]. CHIRPS generates a gridded rain fall time series by combining in-house climatology, CHPclim, 0.05˚ resolution satellite images, and in-situ station data for trend analysis and seasonal drought monitoring. Also, for the atmospheric circulations analysis, daily geopotential height (GPH), Zonal and Meridional wind, RH and Specific humidity was used from the National Centers for Environmental Prediction (NCEP), U. S Department of Energy (DOE) from reanalysis 2 project with horizontal resolution 2.5˚ × 2.5˚ latitude-longitude grid from January 1979 to the present [28].

2.3. Methodology

2.3.1. Data Smoothing

In order to smooth out short-term variations in time series ISV of rainfall, we employed 5-day running mean statistical method [29]. The selection of this method follows its capability of minimizing noise, variability and emphasizes longer-term trends and patterns that might otherwise be hidden [30]. Furthermore, for the sake of identifying patterns, seasonal changes, and anomalies in the data that may not be directly apparent from the raw observations, the smoothed data were plotted alongside the original data for comparison [31].

2.3.2. Dominant Period of Rainfall

Power spectrum analysis was employed to identify the dominant periods of ISV of rainfall. To isolate the ISV of rainfall, a Butterworth band-pass filter was applied. Events with values greater than or equal to 1.0 standard deviation within the 10- to 30-day range were classified as peaks during the ISV of rainfall. A Butterworth low-pass filter method was applied using the bilinear transformation method, which converts the analog filter design into a digital filter [32] (Roberts & Roberts, 1978). The method was achieved by following steps; For the calculation case the squared transfer function, or power gain, is given by the expression

$$\left|H_{B}\left(j\omega\right)\right|^{2}=\frac{1}{1+\left(\omega/\omega_{c}\right)^{2n}} \tag{1}$$

where, ω_c is the cutoff frequency $j=\left(-1\right)^{1/2}$, and n is the number of poles, or order, of the filter. The larger the order, the sharper the cutoff. The subscript B symbolizes the Butterworth transfer function.

A bilinear transformation of (1) produce the corresponding function for discrete system.

$$\left|H\left(j\omega\right)\right|^{2}=\left[1+\left(\frac{\tan\left(\omega T/2\right)}{\tan\left(\omega_{c}T/2\right)}\right)\right]^{-2n} \tag{2}$$

where T is the sampling interval

It is convenient to use the Z transform for discrete systems. The Z transform of a finite data sequence $x_k\left(k=0,1,\cdots,N-1;x_k\equiv 0,k<0\right)$ is denoted by and is defined by

$$Z\left[x_{k}\right]=\sum_{k=0}^{N-1}x_{k}z^{-k}$$

where z is a complex variable. Since for

$$Z\left[x_{k-l}\right]=\frac{x_{0}}{z^{l}}+\frac{x_{1}}{z^{l-1}}+\cdots+\frac{x_{N-1}}{z^{l+N-1}}=z^{-l}Z\left[x_{k}\right] \tag{3}$$

In general, the output $y_k=0$ of any digital filter is given by

$$y_{k}=b_{0}x_{k}+b_{1}x_{k-1}+\cdots+b_{l}x_{k-l}-a_{-1}y_{k-l}-\cdots-a_{n}y_{k-n} \tag{4}$$

$$Y_{z}=H_{(z)}X_{(z)}=\frac{\left(b_{0}+b_{1}z^{-1}+\cdots+b_{l}z^{-1}\right)}{\left(1+a_{1}z^{-1}+\cdots+a_{n}z^{-n}\right)}X_{(z)} \tag{5}$$

The filter coefficients are a_1 and b_1, and is the order of the filter (for non-recursive filters, m is the number of weights, $a_l \equiv 0$, and $n \equiv 0$). Applying the Z transform of both sides of (5), by the convolution theorem, where $Y_{(z)} = Z[y_k], H(z) = Z[h_k]$, and h_n is the impulse response of the filter. The filter coefficients for the Butterworth transfer function may be determined via a bilinear transformation of (3). The study minimizes the roundoff error by flowing the second-order filters. Phase shifts of the signal associate with recursive behavior of Butterworth filter were removed by filtering the signal forward and then backward in time through the same filter. The ISV of rainfall during March, April, and May are obtained by removing the high-frequency and low-frequency variations from the original rainfall time series. This is achieved using the bandpass Butterworth filter method, which isolates the specific frequency range associated with intraseasonal fluctuations. Previous studies such as series [15] [29] [33], have also applied the same methodology.

2.3.3. The Composite Atmospheric Circulation Analysis

The composite method, as described by [34] was utilized to average multiple occurrences of a specific event or phenomenon in order to generate a composite map. Additionally, the 10- to 30-day filtered data for anomalies geopotential height, meridional and zonal wind, RH, OLR and specific humidity was analyzed for the region spanning from 10˚W to 60˚E longitude and 10˚N to 30˚S latitude, with values exceeding 1.0 standard deviations also defined as typical ISV of rainfall events. Following the identification of these typical ISV of events, synthesis analysis and Student's t-test were conducted.

3. Results of the Intraseasonal Variability (ISV) of the Rainfall over Tanzania during MAM Season

3.1. Climatology of Daily Rainfall during MAM Season over Tanzania

Tanzania's climatology during the MAM season was analyzed using CHIRPS observation data from 1983 to 2022. **Figure 2(A)** below illustrates the climatological of daily mean rainfall across the country, oscillating from moderate to high amount (2 to >4 mm/day), with heavy rainfall occurring primarily in western Tanzania, including the Lake Victoria basin and adjacent areas, which receive the highest amount, exceeding 4 mm/day. Central Tanzania experiences moderate rainfall ranging from 2 to 4 mm/day, while southeastern and coastal regions remain drier, with less than 2 mm/day. In March, rainfall begin to increase, particularly in western and central Tanzania, with values ranging between 2 and 4 mm/day, and the Lake Victoria basin and surrounding areas receive relatively higher amount compared to other parts of the country as shown in **Figure 2(B)**. However, coastal and southeastern Tanzania remain dry, with less than 1 mm/day, indicating a delayed onset of the rainy season in these regions. however, coastal and southeastern Tanzania remained significantly dry, with less than 1 mm/day, indicating a delayed onset of the rainy season in these regions. In April, the

eastern, north-eastern, western and Lake Victoria basin indicates the highest amount rainfall > 5 mm/day as shown in Figure 2(C).

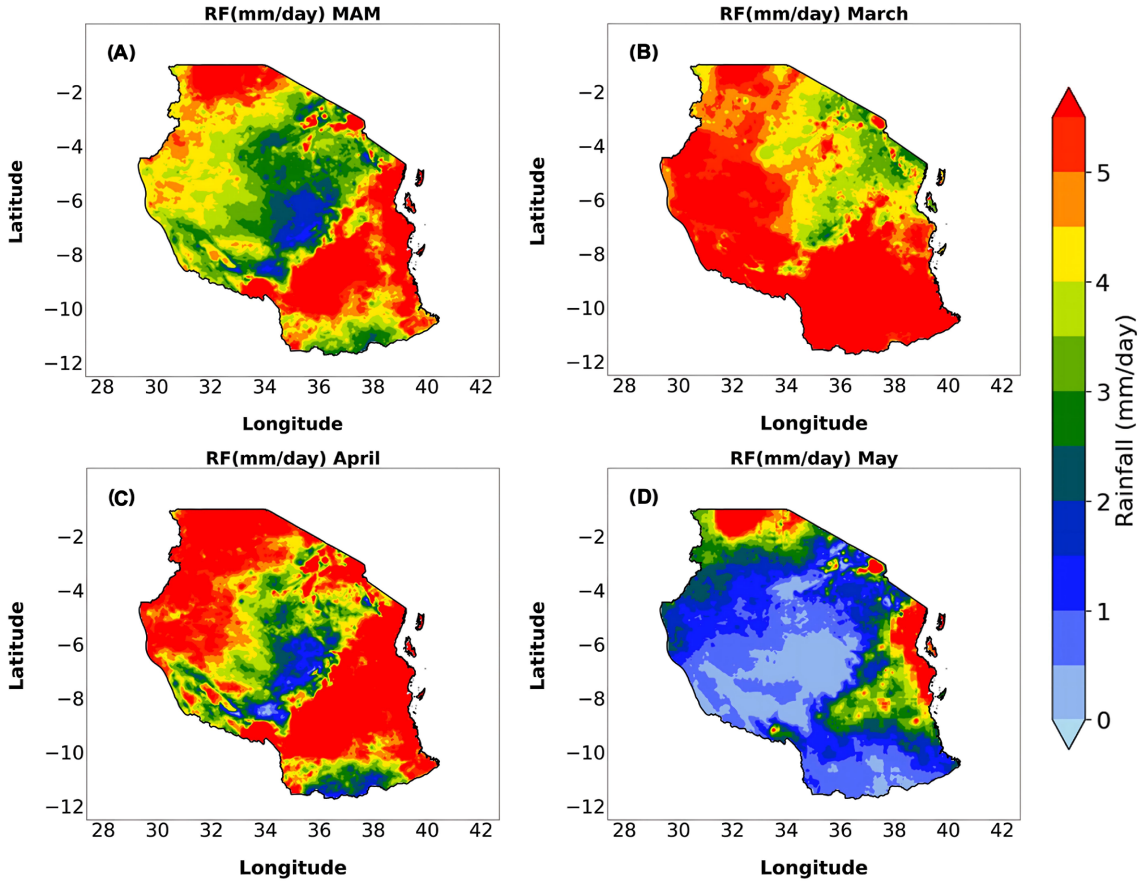

Figure 2. Climatological mean spatial distribution of daily rainfall (mm/day) from CHIRPS data over Tanzania for the MAM season (1983-2022). Panel (A) represents the overall climatological mean for the MAM season, while panels (B), (C), and (D) depict the climatological monthly means for March, April, and May, respectively. The color bar indicates rainfall intensity, with higher values in red and lower values in blue. The patterns highlight regional and temporal variations in rainfall across Tanzania during the MAM season.

In May, the rainy season begin to decrease across most parts of the country; southeastern and southern Tanzania becoming dry, with less than 1 mm/day, while the Lake Victoria basin and northern regions maintain moderate rainfall of 2 to 3 mm/day as shown in Figure 2(D).

3.2. Dominant Peak of ISV over Tanzania during MAM Season of 2022

Investigation of the ISV of the dominant peak over Tanzania of MAM rainfall, was carried out using five day running mean (Figure 3) from the 18 synoptic Meteorological stations observation data from TMA as shown in Figure 1, the bars indicate daily rainfall deviations from the mean average, where positive values show wet conditions and negative values show dry conditions. In March, the ISV of rainfall highlights low rainfall amounts, indicating the beginning of a wet

condition. However, starting from mid-April, the running mean slopes below zero, indicating a shift towards drier conditions that continue through late April and May.

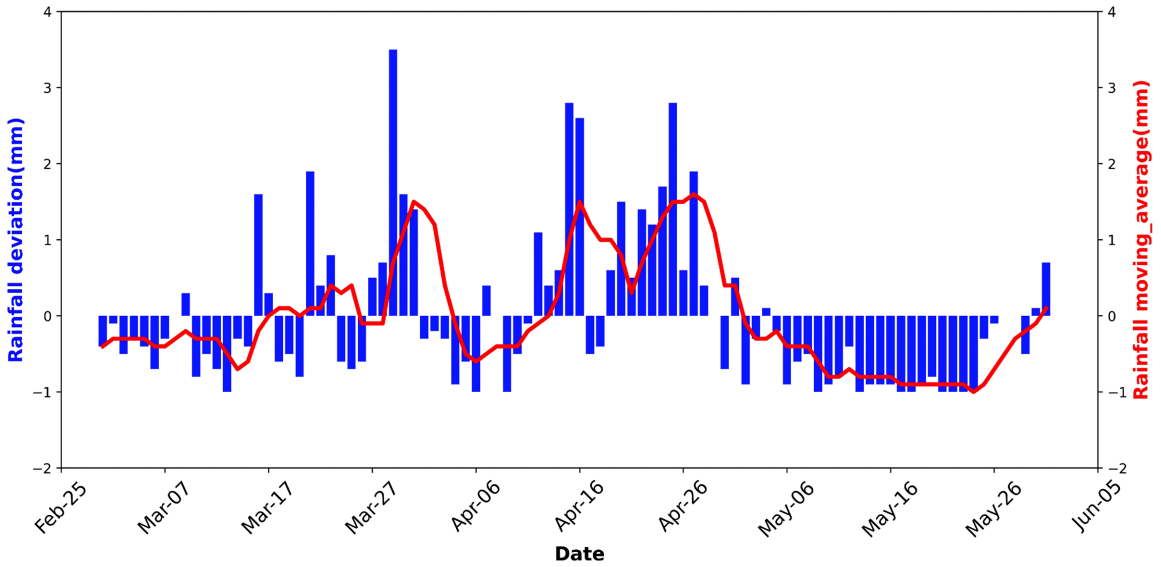

Figure 3. The blue color bar shows time series of the area average of 18 station for Tanzania rainfall MAM of 2022, and red color for the 5-day running mean results depict that there is signal variation of the daily rain fall in study area.

The irregular pattern of positive and negative anomalies indicates the influence of ISV during the MAM season, with these oscillations accounting for the observed variability in rainfall. Also, the Power Spectrum Density was applied to identify the dominant period of rainfall over Tanzania during MAM season in **Figure 4**.

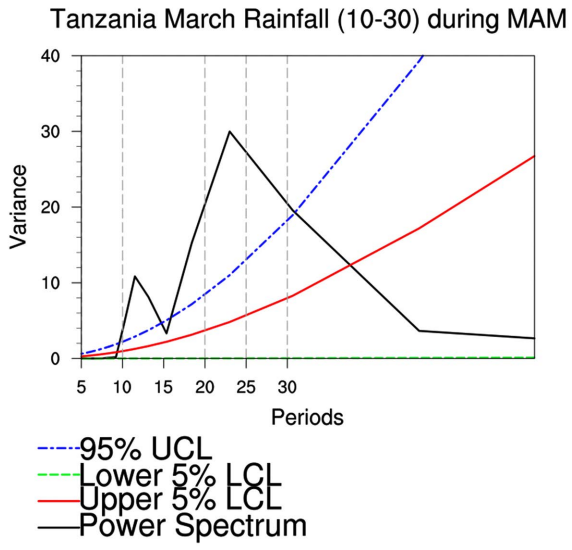

Figure 4. Power spectrum diagram of MAM rainfall in Tanzania average area with 18 observations with data spanning from 2022; of 10 - 30-day filtered rainfall. The black line is the power spectral density, the dashed blue indicates the values of 95% confidence level, the red-line indicates the Upper 5% confidence level and dashed green indicates the 5% lower confidence level.

As shown in Figure 4, the ISV of rainfall during MAM season showed significant a dominant period around the 10 - 25-day, near quasi-biweekly (17 days), which exceeds the 95% Upper Confidence Limit (UCL). The results captured from 10- to 25-day band by Fast Fourier Transform (FFT) within a band of 10 to 30 days range are presented in Figure 5. This curve features distinct peaks that indicates alternating periods of wet and dry days. This pattern aligns with the quasi-biweekly oscillation indicated in (Figure 4) of the Power Spectral Density (PSD), where three peaks in the filtered data mark a cycle of enhanced rainfall, separated by quasi-biweekly intervals as shown in Table 1.

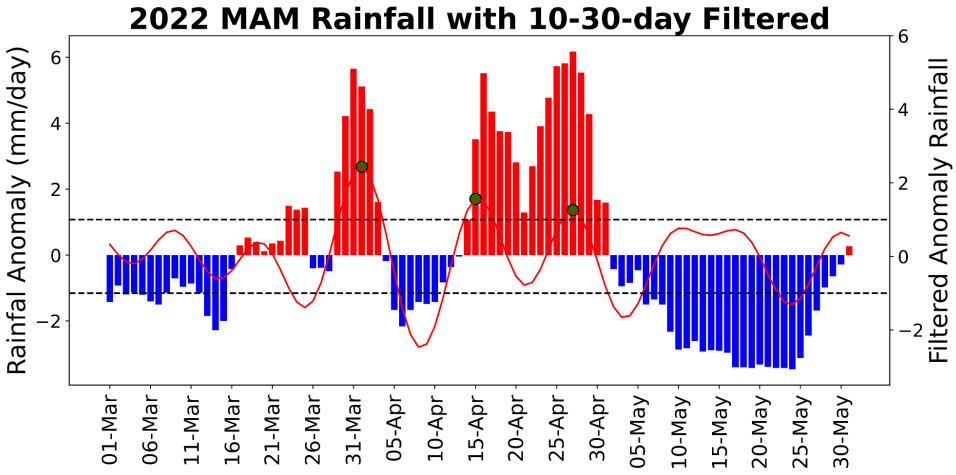

Figure 5. Fast Fourier Transform (FFT) showing the peaks events and indicating the 10 - 30 days filtered with significance of 3 peaks shown by dote green, the black dotted line showing the threshold of select point standard deviation of (+1 to −1), the curved live showing the filtered rainfall, the red bar and blue shows the high and low value of rainfall anomaly.

Table 1. Filtered peak rainfall data table.

Date 1	Peak Event 1	Date 2	Peak Event 2	Date 3	Peak Event 3	Average Peak Event
3/20/2022	−0.1	4/3/2022	−0.4	4/15/2022	1.1	0.2
3/21/2022	−0.6	4/4/2022	−1.4	4/16/2022	0.5	−0.5
3/22/2022	−1.1	4/5/2022	−2.1	4/17/2022	−0.1	−1.1
3/23/2022	−1.4	4/6/2022	−2.5	4/18/2022	−0.7	−1.5
3/24/2022	−1.3	4/7/2022	−2.3	4/19/2022	−0.9	−1.5
3/25/2022	−0.8	4/8/2022	−1.8	4/20/2022	−0.8	−1.2
3/26/2022	−0.1	4/9/2022	−1.0	4/21/2022	−0.4	−0.5
3/27/2022	0.7	4/10/2022	−0.1	4/22/2022	0.1	0.3
3/28/2022	1.6	4/11/2022	0.8	4/23/2022	0.7	1.0
3/29/2022	2.2	4/12/2022	1.4	4/24/2022	1.2	1.6
3/30/2022	2.4	4/13/2022	1.6	4/25/2022	1.3	1.8
3/31/2022	2.2	4/14/2022	1.5	4/26/2022	1.1	1.6

Continued

4/1/2022	1.5	4/15/2022	1.1	4/27/2022	0.6	1.1
4/2/2022	0.6	4/16/2022	0.5	4/28/2022	−0.1	0.3
4/3/2022	−0.4	4/17/2022	−0.2	4/29/2022	−0.8	−0.5
4/4/2022	−1.4	4/18/2022	−0.7	4/30/2022	−1.4	−1.2
4/5/2022	−2.1	4/19/2022	−0.9	5/1/2022	−1.7	−1.6
4/6/2022	−2.5	4/20/2022	−0.8	5/2/2022	−1.6	−1.6
4/7/2022	−2.3	4/21/2022	−0.4	5/3/2022	−1.3	−1.3
4/8/2022	−1.8	4/22/2022	0.1	5/4/2022	−0.7	−0.8
4/9/2022	−1.0	4/23/2022	0.7	5/5/2022	−0.1	−0.3

Furthermore, the analysis in Figure 6 results show that the regional average rainfall intensity reaches 2 mm/day, and quasi-biweekly rainfall occurs 8 days before the peak and lasts for about 8 days.

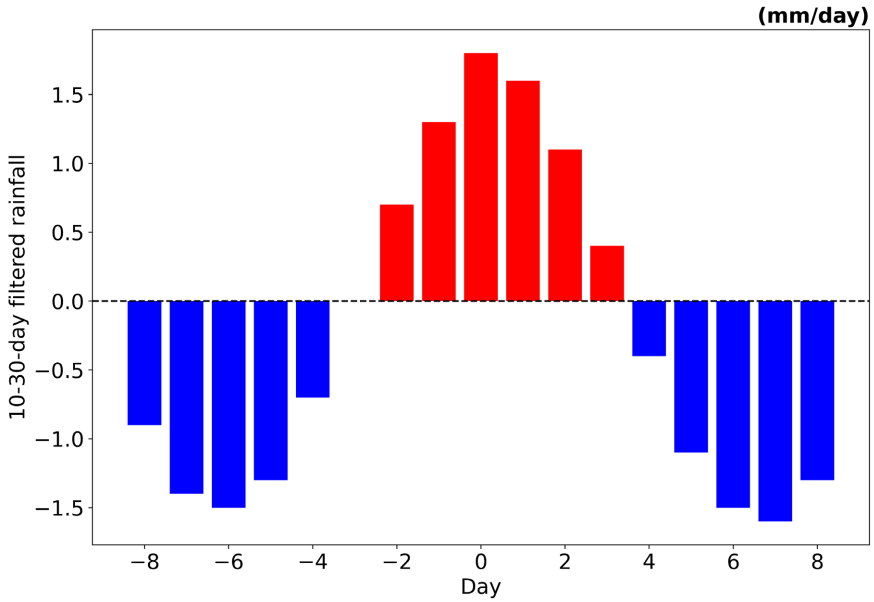

Figure 6. The composite evolution of 10 - 30-days of filtered rainfall over Tanzania During MAM season of 2022.

From the −8-day to the day 0 and then to +8-day phase, the entire cycle takes about 17 days, showing typical intraseasonal variability (ISV) with quasi-biweekly characteristics.

The spatial map sequence of rainfall using CHIRPS data for 2022 during the MAM season reveals the temporal evolution of quasi-biweekly rainfall over around 17 days, from Day −8 to Day +8 in Figure 7. On Day −8 in (Figure 7(A)), negative rainfall anomalies of about −0.5 mm/day persist in the southern and central parts of Tanzania. On Day −6 in (Figure 7(B)), these negative anomalies continue, with a minor decrease in the southern and coastal regions, while central and northern Tanzania rainfall show reductions ranging from −0.8 mm/day to −1.2

mm/day. On Day −4 in (Figure 7(C)), indicates positive rainfall anomalies of around (0.5 to 0.8 mm/day) in southern and central Tanzania, while northwest region was observed to have minimum rainfall anomalies between (−0.8 and −1.2 mm/day). The positive anomalies increase to about (0.8 to 1 mm/day), signifying a transition to higher rainfall levels on Day −2 in Figure 7(D). The peak of the active rainfall phase occurs on Day 0 in (Figure 7(E)), with significant positive anomalies indicating an increase rainfall anomaly around (0.8 mm to 2 mm/day) over Tanzania, but weak rainfall anomalies in the central, southern, and parts of the eastern regions. On Day +2 in Figure 7(F), positive anomalies are observed in the coastal region, central, and western parts of Tanzania, although with a slight reduction in intensity, show the beginning of a reduced rainfall phase. On Day +4 in Figure 7(G), negative rainfall anomalies of about −0.8 mm/day indicate a return to drier conditions, while the spatial extent of positive anomalies continues to decrease.

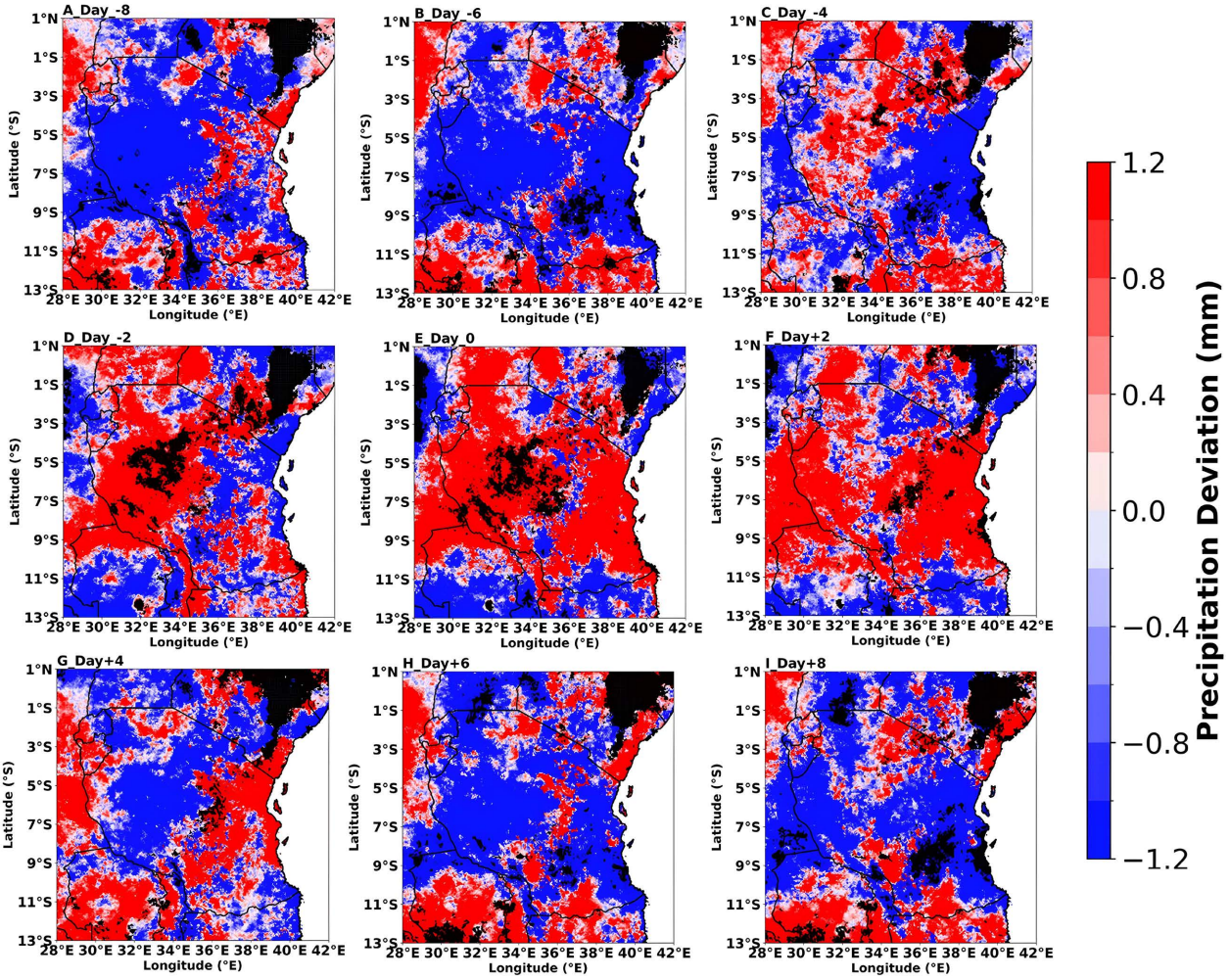

Figure 7. Shows the composite evolution of 10 - 30-day filtered rainfall anomalies (unit: mm/day) across Tanzania during the MAM season of 2022, from day −8 to day +8. Each subplot detentions rainfall deviations, with red areas indicating positive anomalies (wet date) and blue areas representing negative anomalies (dry date). Black dots signify regions where rainfall anomalies are statistically significant at the 95% confidence level, based on a t-test.

The negative anomalies fluctuate more in (Figure 7(H) of Day +6, with lower rainfall anomalies around (−0.8 to −1.2 mm/day) in central and northern regions. In (Figure 7(J) of Day +8, negative anomalies dominate at large regions of Tanzania, showing a return to dry phase.

4. Influences of Atmospheric Circulation on ISV

After the examination of the dominant mode of intraseasonal variability (ISV) of rainfall over Tanzania during the MAM season, the analysis was further extended to investigate the atmospheric circulation mechanisms including Geopotential Height, RH, Wind systems, OLR and Moisture Flux interact with ISV.

4.1. Effect of Geopotential Height and Wind Anomalies at 850 hPa Low Level Circulation and 200 hPa

The composite maps of geopotential height anomalies and wind at the 850 hPa level (Figure 8) revealed an irregular pattern of convergence and divergence that modulates the ISV of rainfall over Tanzania, as indicated within the red box.

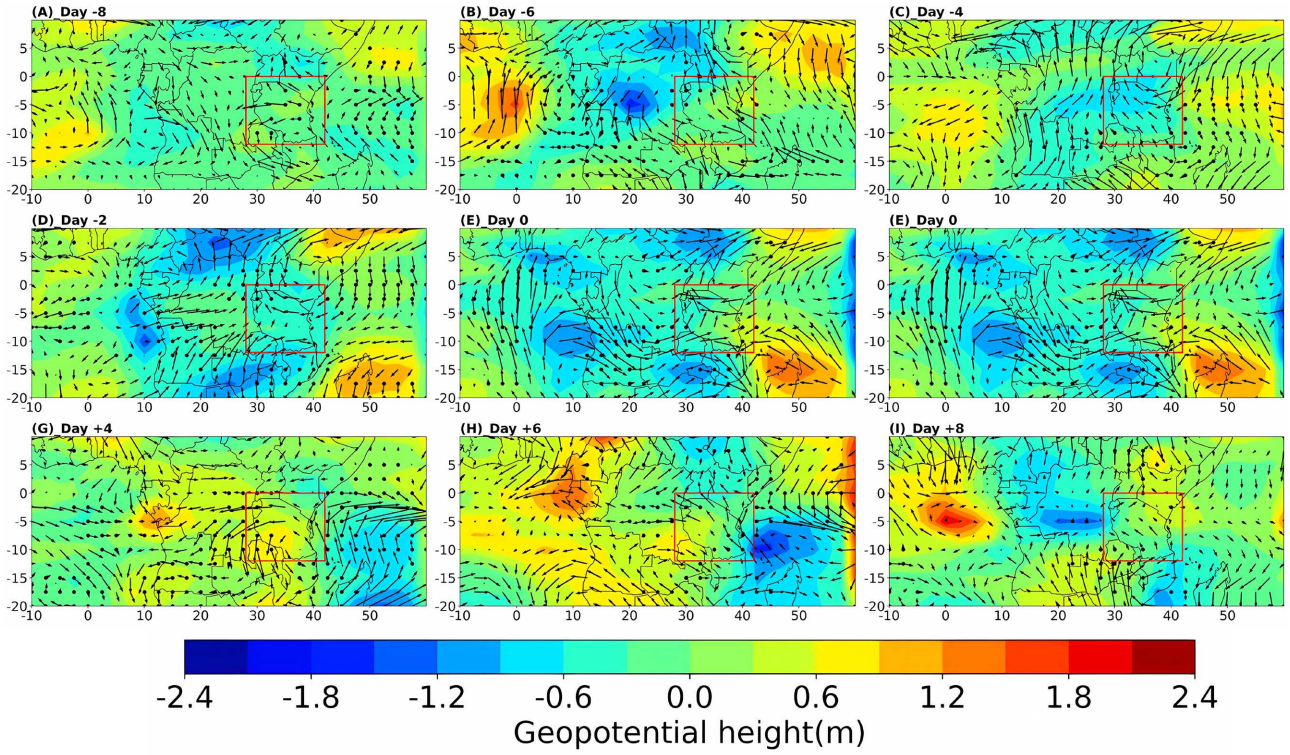

Figure 8. Composite distribution of geopotential height anomalies (color shaded, unit's m, dotted black is significantly of >95%) at 850 hPa and wind vectors (vector, unit's: m/s) at the 850 hPa level, filtered 10- to 30-day intraseasonal oscillations. This based on the region between 10˚W to 60˚E longitude and 30˚S to 10˚N latitude, covering East Africa, the Congo Basin, the western Indian Ocean, and the Mozambique Channel. The study area is marked by a red box over Tanzania, where we observe the factors contributing to rainfall variability.

The results show negative geopotential height anomalies observed at lag −8 and lag −6 (Figure 8(A), Figure 8(B)), ranging from −0.3 to −0.7 m, over the Western

Indian Ocean (10˚S to 15˚S, 40˚E to 50˚E) and the Mozambique Channel (20˚S to 10˚S, 30˚E to 40˚E). These anomalies promote low-level convergence and moisture inflow into the Tanzania region, overlapping with converging wind patterns that support upward motion and convection. The results indicate that these negative anomalies increase to approximately −0.5 to −0.8 m at lag −4 (**Figure 8(C)**), leading to an increase in low-level convergence and rainfall. At lag −2 (**Figure 8(D)**), a transition to neutral or positive anomalies in the Western Indian Ocean and Mozambique Channel reduces moisture transport. However, rising negative anomalies over Southern Africa (15˚S to 25˚S, 20˚E to 30˚E) induce upward motion, further enhancing convection over Tanzania. At lag 0 (**Figure 8(E)**), strong negative anomalies ranging from −0.57 to −1.14 m persist over Southern Africa (15˚S to 25˚S, 20˚E to 30˚E) and the surrounding regions. These anomalies converge with winds from the Western Indian Ocean and Mozambique Channel, creating optimal conditions for peak rainfall. From lag +2 (**Figure 8(F)**), results reveal a positive anomaly of about 0.2m to 1.4m observed over Tanzania resulting in low-level divergence and reduced rainfall, while weak negative anomalies in the Congo Basin (5˚S to 10˚S, 15˚E to 25˚E) resulted in limited moisture and reduced convergence to the west, with shifting rainfall away from the region. At lag +4, +6, and +8 (**Figures 8(G)-(I)**), strong positive anomalies of approximately (0.6 to 1.6 m) were observed over the study region, resulting in dry conditions. **Figure 9** illustrates the pattern of geopotential height anomalies and upper-level wind patterns (200 hPa) across East Africa, including Tanzania. The results indicate that at lag −8 (**Figure 9(A)**), strong negative geopotential height anomalies of around −1.5 m to −2.25 m dominated the Mozambique Channel (20˚S to 10˚S, 30˚E to 40˚E), which was associated with the development of cyclonic circulation. In addition, a positive anomaly observed in the range of 0.57 to 1.14 m over Tanzania, resulted in weak upper-level divergence, indicating the starting phase of rainfall. At lag −6 (**Figure 9(B)**), the results show that positive anomalies increase over Tanzania, enhancing upper-level divergence and downward wind. At the same time, cyclonic winds over the Mozambique Channel facilitate moisture transport. At lag −4 (**Figure 9(C)**), positive anomalies continue to strengthen over Tanzania, as indicated by the red box, increasing upper-level divergence. Meanwhile, negative anomalies in the Western Indian Ocean (10˚S to 0˚, 50˚E to 60˚E) drive cyclonic winds, enhancing monsoon flow toward Tanzania. At lag −2 (**Figure 9(D)**), positive anomalies (ranging from approximately 1.14 to 1.71 m) persist over Tanzania, maintaining upper-level divergence and favorable conditions for convection, while the influence of negative anomalies in the Mozambique Channel diminishes.

At lag 0 (**Figure 9(E)**), positive anomalies peak (approximately 0.7 m to 2.0 m) over Tanzania (as indicated by the red box), coinciding with the date of peak ISV rainfall. This strong upper-level divergence is associated with significant upward motion and favorable moisture transport from the Western Indian Ocean. After the peak date at lag +2 (**Figure 9(F)**), the results indicate that the positive anomalies start to weaken slightly (about 0.5 m to 1 m) over Tanzania, which leads to

reduced upper-level divergence and convection, meanwhile negative anomalies (around −1.14 to −2.25 m) increase over the Congo Basin (5˚S to 10˚S, 15˚E to 25˚E), which shifts divergence and rainfall westward. At lag +4 (Figure 9(G)), positive anomalies over Tanzania weaken further, suppressing upward motion, while strong negative anomalies dominate the Congo Basin, enhancing upper-level divergence and rainfall in that region. At lag +6 (Figure 9(H)), positive anomalies over Tanzania are further reduced, leading to dry conditions, as intensifying negative anomalies over the Congo Basin drive strong upper-level divergence and rainfall activity. At lag +8, strong negative anomalies over Tanzania and strong negative anomalies over the Congo Basin, simultaneously continue to sustain upper-level divergence and rainfall, resulting in dry conditions in Tanzania.

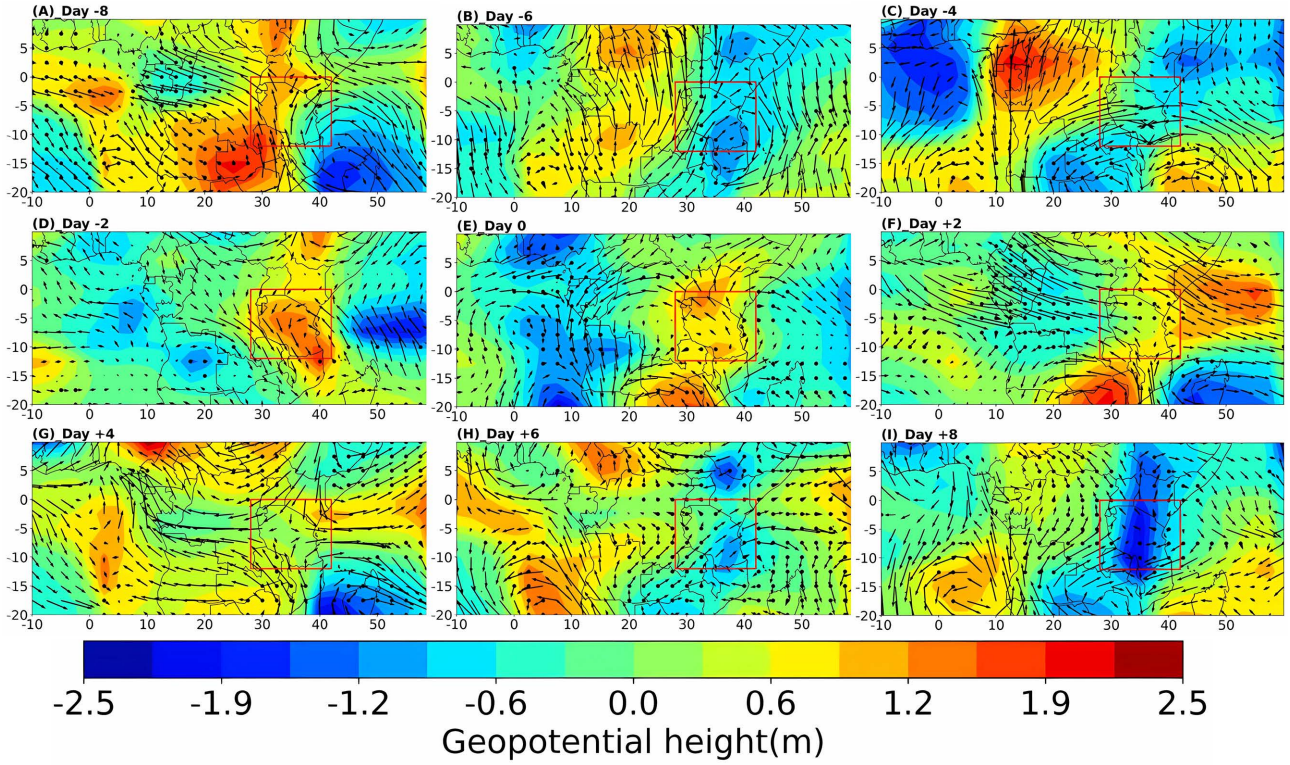

Figure 9. Composite distribution of geopotential height anomalies (color shaded, unit: m, the dotted black circle is significantly of >95%) at 200 hPa and wind vectors (vector, unit: m/s) at the 200 hPa level, filtered 10- to 30-day intraseasonal oscillations. This based on the region between 10˚W to 60˚E longitude and 30˚S to 10˚N latitude, covering East Africa, the Congo Basin, the western Indian Ocean, and the Mozambique Channel. The study area is marked by a red box over Tanzania, where we observe the factors contributing to rainfall variability.

4.2. Effects of Relative Humidity (RH) and Wind Anomalies at 850 hPa and 200 hPa on ISV

The composite analysis of 10 - 30-day intraseasonal oscillations show the significant role of RH anomalies and wind patterns at 850 hPa in influencing the ISV of rainfall in Tanzania during the MAM season. This analysis underlines the complex relationships among moisture transport, convergence, and wind dynamics, as represented in Figure 10.

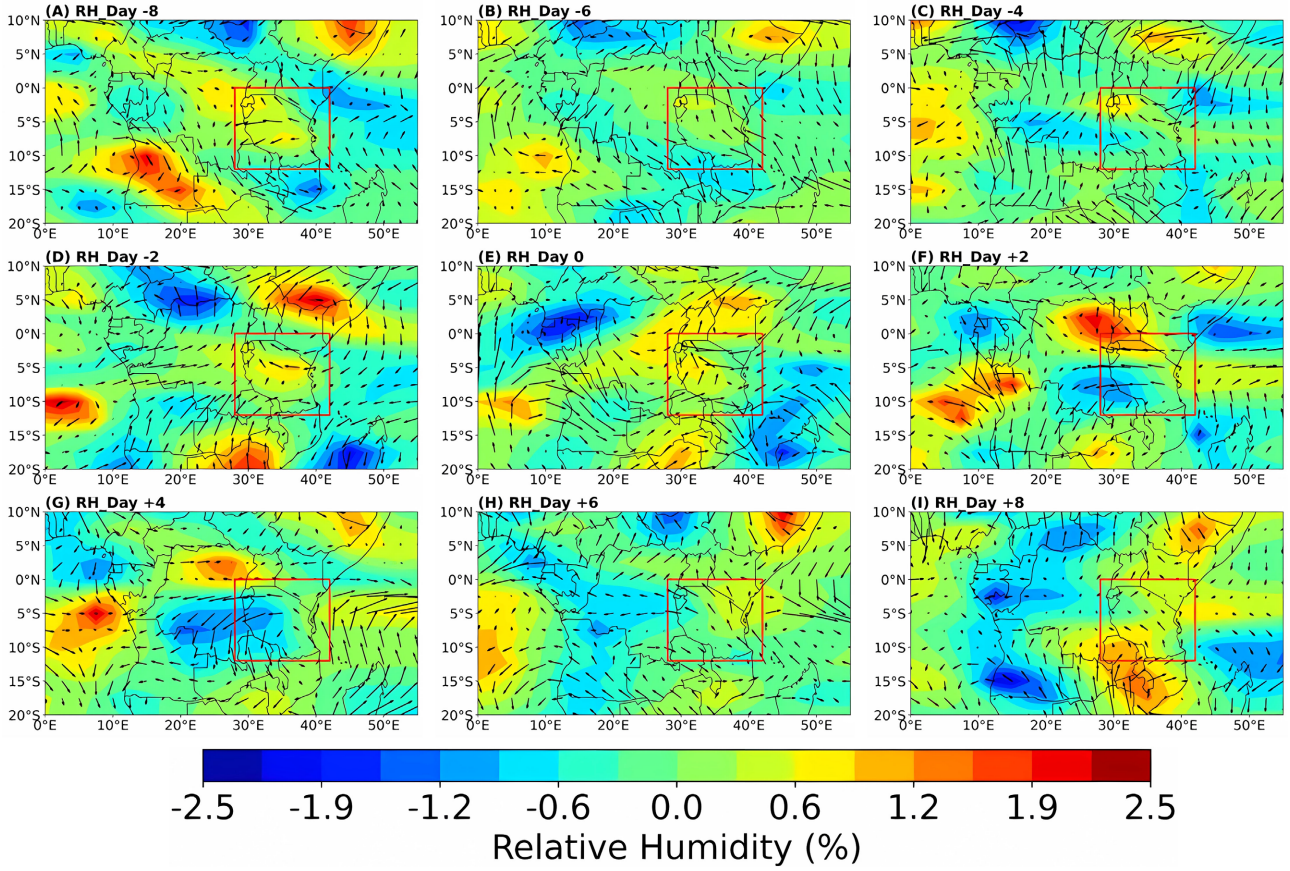

Figure 10. Composite distribution of RH anomalies (color shaded, unit, %, dotted black is significantly of >95%) at 850 hPa and wind vectors (vector, unit's m/s) at the 850 hPa level, filtered 10- to 30-day intraseasonal oscillations. This based on the region between 10˚W to 60˚E longitude and 30˚S to 10˚N latitude, covering East Africa, the Congo Basin, the western Indian Ocean, and the Mozambique Channel. The study area is marked by a red box over Tanzania, where we observe the factors contributing to rainfall variability.

On Day −8 (Figure 10(A)), the region experiences dominant negative RH anomalies (−0.5% to −0.8%), characterized by weak low-level westerly winds originating from the Congo Basin and northerly winds that bring dry air into Tanzania, thereby restricting moisture transport. On Day −6 (Figure 10(B)), positive anomalies begin to rise (0.5% to 0.65%) to the west of Tanzania, driven by strengthening low-level westerly winds from the Congo Basin and easterly winds from the Indian Ocean, indicating an initial accumulation of moisture. On Day −4 (Figure 10(C)), these positive anomalies strengthen further as westerly winds enhance moisture transport from the Congo Basin, while easterly winds converge over Tanzania, leading to significant accumulation of moisture. On Day −2 and Day 0 (Figure 10(D), Figure 10(E)), results show that positive anomalies peak at (0.8% to 1.0%) due to strong low-level convergence of westerly and easterly winds at 850 hPa, which enhanced vertical motion and rainfall. The dry phase begins on Day +2 (Figure 10(F)), marked by the onset of negative anomalies (−0.5% to −0.7%) resulting from the weakening of low-level winds and the introduction of northerly winds that bring dry air into the region. On Day +4 (Figure 10(G)),

negative anomalies prevail (−0.8% to −1.0%), indicating reduced moisture transport and divergence, signifying the peak of the dry phase. On Day +6 (Figure 10(H)), negative anomalies begin to weaken as westerly winds regain strength west of Tanzania, suggesting a gradual shift back to wetter conditions. Finally, on Day +8 (Figure 10(I)), positive anomalies reappear over the Congo Basin and the western Indian Ocean, coinciding with renewed convergence of low-level westerly and easterly winds over Tanzania, showing the initial phase of ISV.

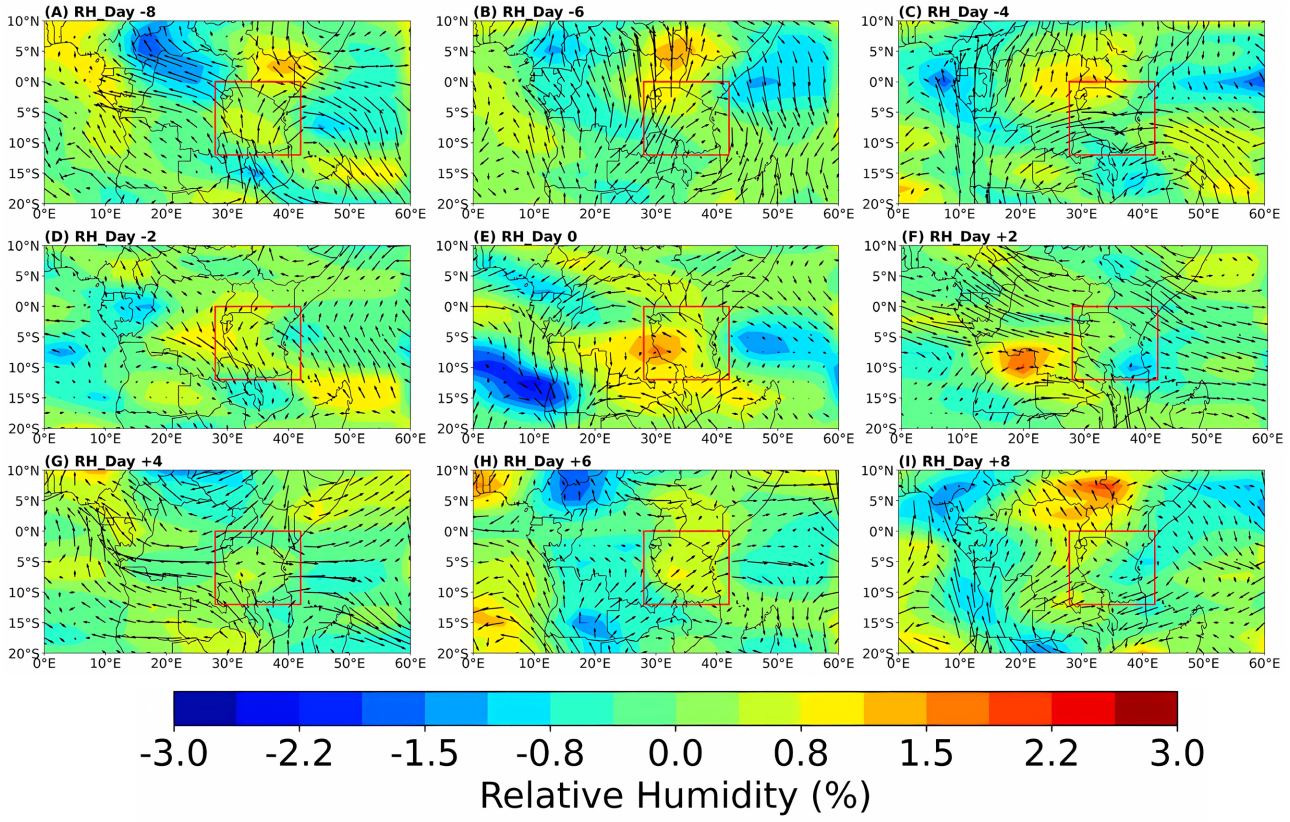

Figure 11. Composite distribution of RH anomalies (color shaded, unit, %, dotted black is significant of >95%) at 200 hPa and wind vectors (vector, unit m/s) at the 200 hPa level, filtered 10- to 30-day intraseasonal oscillations. This based on the region between 10˚W to 60˚E longitude and 30˚S to 10˚N latitude, covering East Africa, the Congo Basin, the western Indian Ocean, and the Mozambique Channel. The study area is marked by a red box over Tanzania, where we observe the factors contributing to rainfall variability.

This ISV of quasi-biweekly observations illustrates Tanzania's transition from moisture-rich conditions with wet to dry conditions, influenced by alternating periods of convergence and divergence, as shown in Figure 11. On Day −8 (Figure 11(A)), positive RH anomalies (1% to 1.5%) dominate over the Congo Basin and western Indian Ocean, while Tanzania exhibits weak positive anomalies of approximately (0.2% to 0.5%). Wind patterns reveal upper-level divergence over these moisture-rich areas, indicating initial condition for moisture transport towards Tanzania, which remain in an initial phase. On Day −6 (Figure 11(B)), positive RH anomalies (0.5% to 1%) spread eastward, with slight increase over Tanzania, while stronger anomalies persist in the Congo Basin and western Indian

Ocean. Divergence increases over the western Indian Ocean and East Africa, extending towards Tanzania, enhancing instability. On Day −4 (Figure 11(C)), positive RH anomalies intensify over Tanzania, supported by strong upper-level divergence and significant upward motion, marking a high-potential phase for rainfall. On Day −2 in (Figure 11(D)), RH anomalies peak at up to 1.5% over Tanzania, with strong divergence further enhancing upward motion.

On Day 0 (Figure 11(E)), positive RH anomalies (+0.5% to +2%) dominate Tanzania, while the western Indian Ocean continues to contribute moisture. As the days progress, from Day +2 to Day +8 in (Figure 11(F), Figure 11(G)), positive RH anomalies gradually weaken over Tanzania and shift eastward, with the western Indian Ocean becoming increasingly dominant in supporting moisture, this shift leads to a decrease in rainfall for Tanzania as it shifts into a neutral to less active phase on Day +8 (Figure 11(I)).

4.3. The Impacts of Outgoing Long Wave Radiation (OLR) Anomalies on ISV

Tanzania region experienced significant positive OLR anomalies of around 10-15 W/m^2, as shown in Figure 12(A) and Figure 12(B) at Lag −8 and Lag −6, indicating a decrease in cloud cover and convection. These results show the initial phase of ISV of rainfall, as moisture inflow from the Congo Basin, Mozambique Channel, and SWIO was minimal. At Lag −4 (Figure 12(C)), the OLR anomalies were neutral to low negative, approximately 0 to −5 W/m^2.

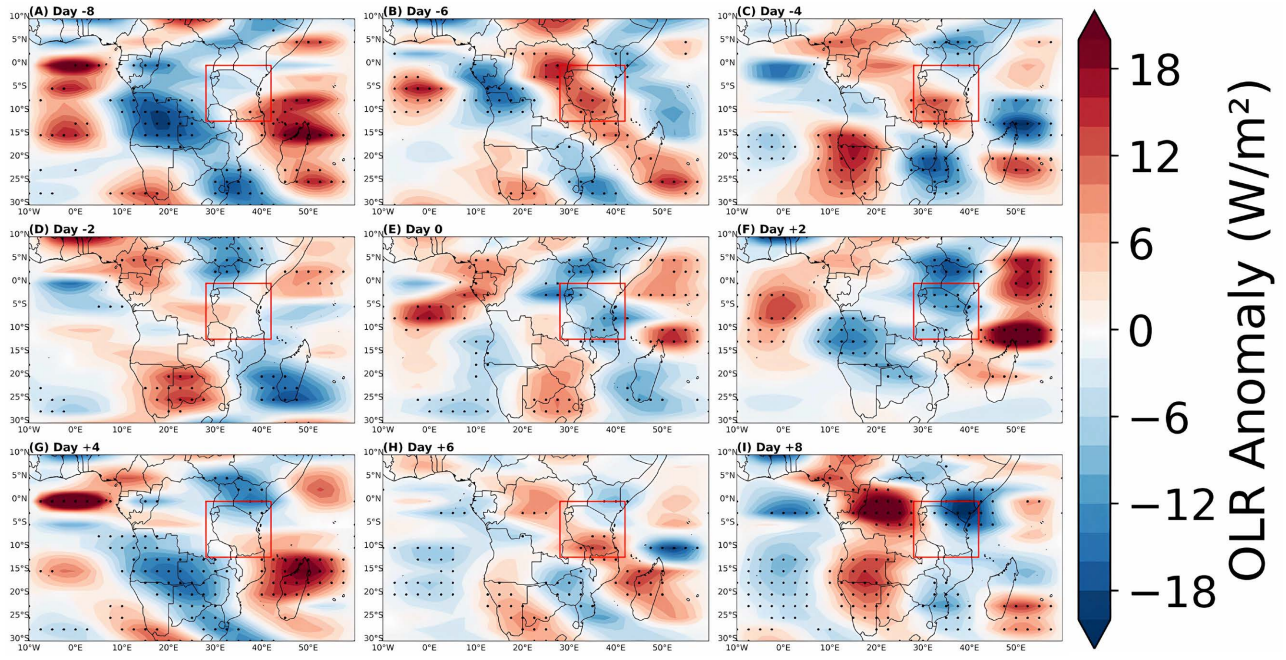

Figure 12. Composite distribution of Outgoing Longwave Radiation (OLR) anomalies (shaded, in W/m^2) filtered to the 10 - 30-day intraseasonal oscillations, averaged over specific days relative to key rainfall events in the MAM 2022 season. The black dotted areas indicate statistically significant anomalies at the 95% confidence level. The analysis spans a domain from 10˚W to 60˚E longitude and 30˚S to 10˚N latitude, surrounding East Africa, the Congo Basin, the western Indian Ocean, and the Mozambique Channel. The study focus region, marked with a red box, highlights Tanzania, where the impact of OLR variability on rainfall patterns is explored.

This change resulted in stronger moisture accumulation on the western side of Tanzania near the Congo Basin and increased convection in both the Mozambique Channel and SWIO. At Lag −2 (Figure 12(D)), Tanzania entered a peak wet phase, experiencing minimum moisture in the region and significant low rainfall. At Lag 0 (Figure 12(E)), which corresponds to the peak date of rainfall, the results show significant negative OLR values of around −18 W/m^2 to −20 W/m^2, and moisture convergence reached its highest point, resulting in heavy rainfall. After the peak date, negative OLR values continued to persist over Tanzania at Lag +2 (Figure 12(F)) and in the southwest near the Congo Basin. However, along the longitude from 40˚E to 50˚E, strong positive OLR values of 10 W/m^2 to 15 W/m^2 were observed, leading to decreased moisture contributions from surrounding areas. From Lag +4 to Lag +6 (Figure 12(G-H)), positive OLR anomalies dominated, resulting in a stable dry phase characterized by high positive OLR. At lag +8 (Figure 12(I)), a weak negative OLR was observed along the red box region, indicating the start of another initial wet phase.

4.4. Composite of Vertical Section of the Zonal Wind and Meridional Wind Average Latitude along (12˚S to 0)

In the wet phase (Figure 13(A)), strong westerlies between 0˚ and 20˚E longitude exhibit positive anomalies up to 1.8 m/s in the mid-troposphere (300 - 600 hPa), bringing moist air from the Indian Ocean and driving convection. Additionally, easterlies between 30˚ and 50˚E longitude at 400 - 700 hPa, with anomalies reaching −1.0 m/s, represent air from the Congo region, contributing to convection. This interaction between the westerlies and easterlies promotes moisture convergence and upward motion, creating favorable conditions for rainfall and low-pressure development.

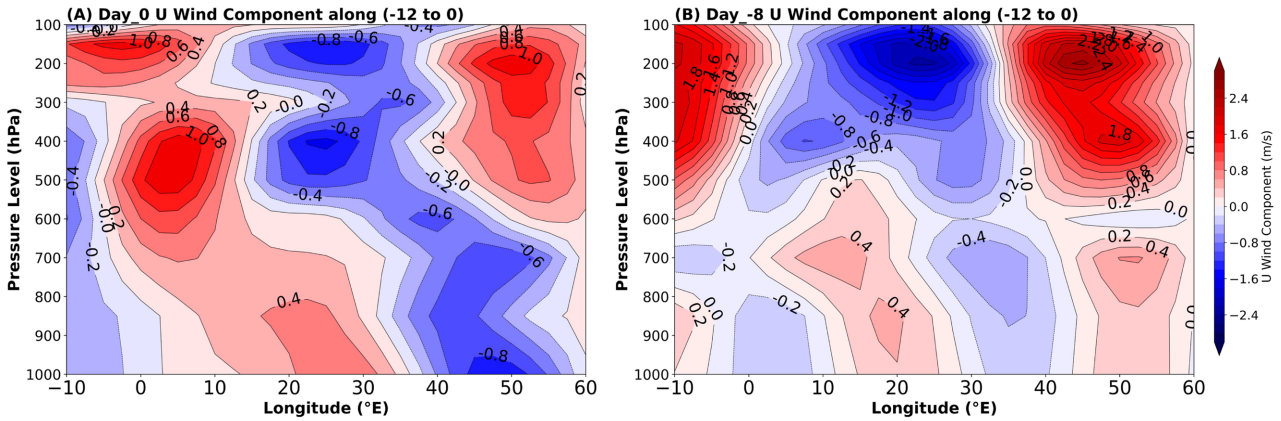

Figure 13. Show two composite vertical sections of zonal wind anomalies along 12˚S to 0˚ latitude, Day 0 (peak wet phase) on the left panel (A) and Day −8 (dry phase) on the right panel (B). The anomalies are in m/s, with positive values (red shades) representing westerly anomalies and negative values (blue shades) indicating easterly anomalies. The dashed contour lines represent easterly winds, with intervals of 0.2 m/s.

In the dry phase (Figure 13(B)), dominant westerlies between 0˚ and 20˚

longitude, reaching up to 2.4 m/s at 200 - 500 hPa, indicate stable atmospheric conditions. Weaker, irregular easterlies at 30˚ to 50˚ longitude and 600 - 900 hPa provide minimum support for convection. This stable pattern of strong westerlies and weak easterlies disrupts interaction, reducing moisture influx and upward motion, which limits rainfall and low-pressure formation, ultimately resulting in the dry phase. Figure 14(A) results illustrate the wet phase of the ISV of rainfall during peak date, with significant southerly winds between 0˚ and 10˚E longitude and around 40˚ to 50˚ longitude in the mid-troposphere (300 - 500 hPa), peaking approximately 2.4 m/s. These southerly anomalies transport warm, moist air northward, promoting moisture convergence and enhancing convective activity. Meanwhile, rapid northerly anomalies observed between 10˚ and 30˚ longitude, with strengths reaching −2.4 m/s, introduce cooler air from 100 to 600 hPa. The interaction between these opposing wind anomalies creates a dynamic that intensifies convergence and convection, resulting in heavy rainfall in Tanzania during the MAM season. Conversely, Figure 14(B) depicts the dry phase, characterized by strong southerly anomalies (up to 4.0 m/s) dominating between 0˚ and 30˚ longitude, extending from the surface to near 200 hPa.

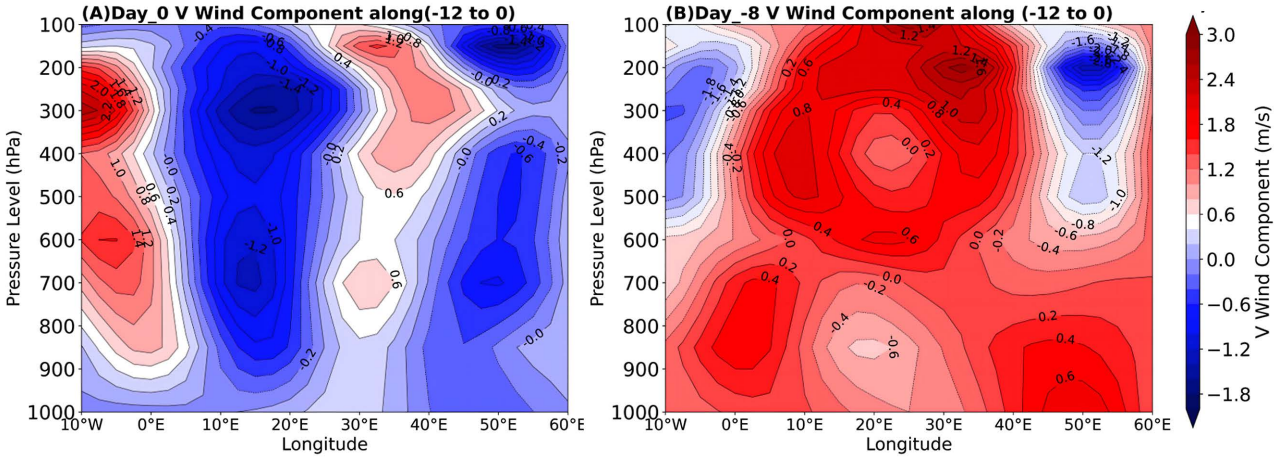

Figure 14. Show the Day 0 (wet phase) and Day −8 (dry phase) filtered 10 - 30-day meridional wind anomalies (unit: m/s) average along 12˚S to 0˚ latitude, with a specific focus on Tanzania (longitude 28˚ to 42˚) during the March-April-May (MAM) season.

This stable layer of warm air limits moisture mixing and suppresses convective processes, while weak northerly anomalies are confined to the 50˚ - 60˚ longitude range at upper levels (above 200 hPa), providing minimal cool air invasion. The predominance of strong southerly anomalies, combined with the absence of significant northerly anomalies, creates unfavorable conditions for rainfall, leading to low rainfall in Tanzania and East Africa during the MAM season.

4.5. Composite of Map Sequence of the Water Vapor Flux (WVF) Anomalies Integrated at 500 hPa

The composite map pattern for water vapor flux (WVF) at 500 hPa was analyzed to assess moisture transport, revealing significant influences on convective

development over Tanzania, as shown in Figure 15. At Lag −8 to Lag −6 (Figure 15(A), Figure 15(B)), the results indicate weak positive moisture around 0.2 kg/kg·m/s over Tanzania, primarily dominated by flow from the southeastern moisture flux, with minimal contributions from the Indian Ocean. The mid-level moisture transport contributes little to convective activity. The positive WVF anomalies increase slightly to around 0.4 kg/kg·m/s along the 10˚S - 15˚S band at Lag −4 to Lag −2 (Figure 15(C), Figure 15(D)).

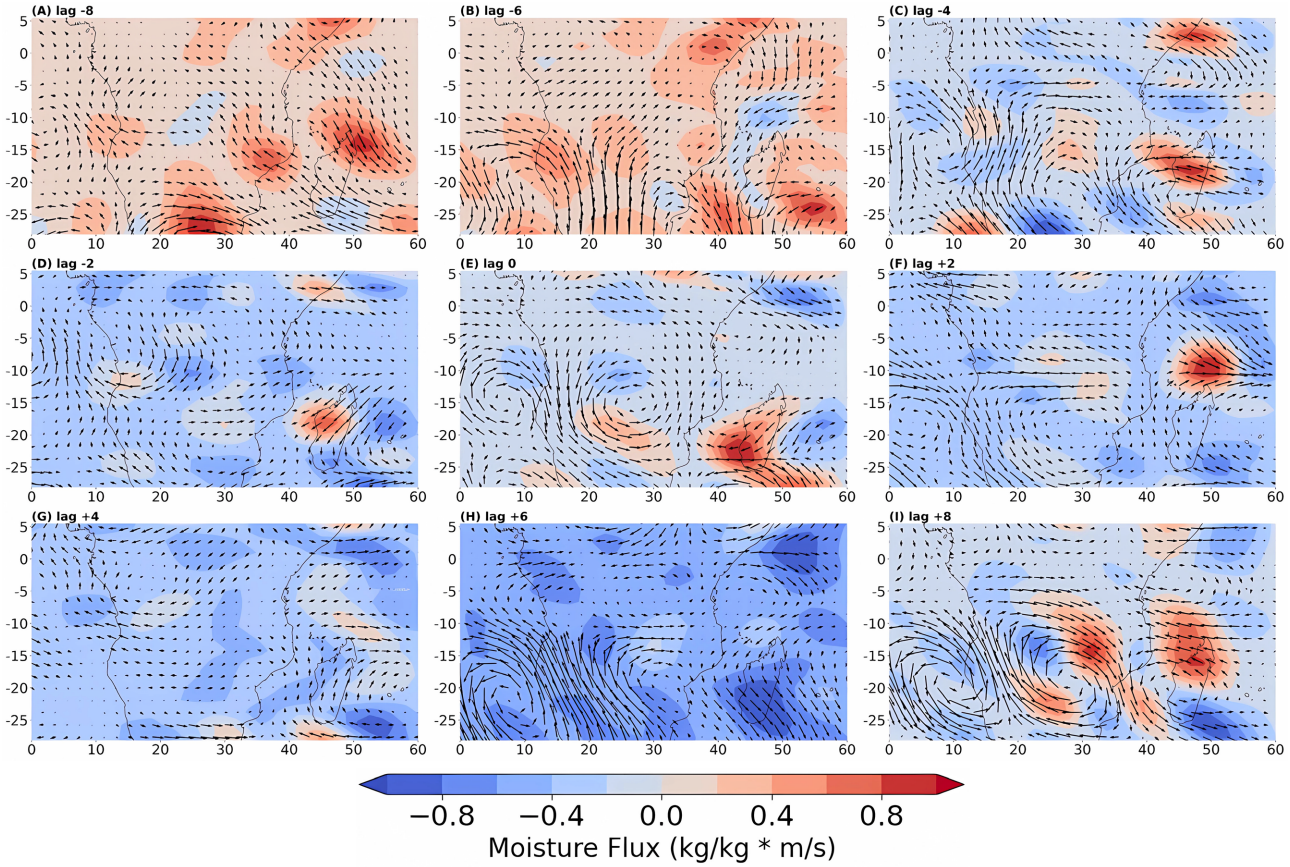

Figure 15. Composite map sequences of the water vapor flux at 500 hPa for Day −8, to +8, filtered for 10 - 30-day intraseasonal variability (ISV) of quai-biweekly. The nine sub-plots, labeled A, B, C to I, each panel shows moisture flux (kg/kg*m/s) in color shading and wind vectors indicating moisture flux direction and strength.

The results show that inflow from the northeastern sector strengthens, interacting with weak flow from the southeastern region near Madagascar. Convergence over Tanzania remains weak but begins to form, signifying an accumulation of mid-level moisture conducive to convection. At Lag 0 (Figure 15(E)), significant positive moisture flux anomalies are observed over Tanzania and East Africa, with values ranging from +0.4 to +0.8 kg/kg·m/s. A clear increase in moisture convergence is evident in the region. Moreover, a well-defined cyclonic anomaly in the Mozambique Channel is noted, which is transporting moisture from the Indian Ocean. Westerly winds are also present, enhancing the transport of moisture direct into the area. Positive moisture flux anomalies persist at Lag +2 (Figure

15(F)) but weaken to around +0.2 to +0.4 kg/kg·m/s, suggesting reduced moisture inflow. Over the Mozambique Channel, cyclonic circulation continues, but its strength diminishes, and westerly winds weaken, indicating a gradual decline in moisture transport over Tanzania. At Lag +4 (Figure 15(F)), neutral to weak positive moisture flux anomalies suggest a shift toward suppressed conditions, with cyclonic circulation over the Mozambique Channel dispersing and winds over Tanzania becoming easterly, marking the transition to a suppressed phase. At Lag +6 (Figure 15(G)), negative moisture flux anomalies develop over Tanzania and East Africa, signifying suppressed moisture inflow, while signs of anticyclonic circulation return over the Southwest Indian Ocean. At Lag +8 (Figure 15(I)), strong negative moisture anomalies (−0.4 to −0.8 kg/kg·m/s) dominate over Tanzania and East Africa, reflecting blocked moisture transport, as a fully restored anticyclonic anomaly limits moisture advection over the SWIO and intensifies easterly winds over Tanzania, further suppressing moisture transport.

4.6. The Influences of Wind Anomalies at Level 850 hPa and 200 hPa on ISV

Figure 16 shows that the irregular patterns of convergence and divergence drive the intraseasonal variability (ISV) of quasi-biweekly oscillations in rainfall, with a roughly 17-day cycle that reflects periodic shifts in moisture transport and atmospheric stability over Tanzania. On Day −8 (Figure 16(A)), there is a weak northeasterly wind around 30˚E to 40˚E and 5˚S to 10˚S, while southeasterly winds from the Indian Ocean (40˚E to 55˚E, 5˚S to 15˚S) dominate the coastal region. As time evolves, as observed in (Figure 16(B)) on Day −6, the southeasterly winds strengthen and move inland, resulting in low-level convergence around 35˚E and 5˚S to 10˚S, signifying the start of a transition toward improved convective potential. On Day −4 (Figure 16(C)), the results show that convergence strengthens over Tanzania, around 30˚E and 40˚E, and 5˚S to 5˚N, due to interactions between northwesterly flows from the Congo Basin (10˚E to 30˚E, 5˚S to 5˚N) and southeasterly winds from the Indian Ocean.

The peak occurs on Day 0 (Figure 16(E)), where strong southeasterly winds converge with northwesterly winds over central Tanzania (30˚E to 40˚E and 5˚S to 10˚S), supporting important moisture transport and enhanced convective activity, leading to increased rainfall. This convergence is strong over the Tanzanian region, contributing to rainfall peaks associated with quasi-biweekly oscillations. Following this peak, on Day +2 in Figure 16(F), convergence begins to weaken as southeasterly winds decrease, marking the start of a drier phase. Divergence patterns become more pronounced on Day +4 to Day +8 in (Figures 16(G)-(I)), with southeasterly winds extending farther inland without strong opposing flows from the northwest, particularly around 40˚E and 5˚S to 15˚S. On Day −8 (Figure 17(A)), significant divergence is observed around 30˚E - 40˚E and 5˚S - 5˚N, suggesting dry upper-level conditions that suppress convection over Tanzania. This pattern continues through Day −6 (Figure 17(B)), with sustained divergence and limited moisture inflow from nearby regions.

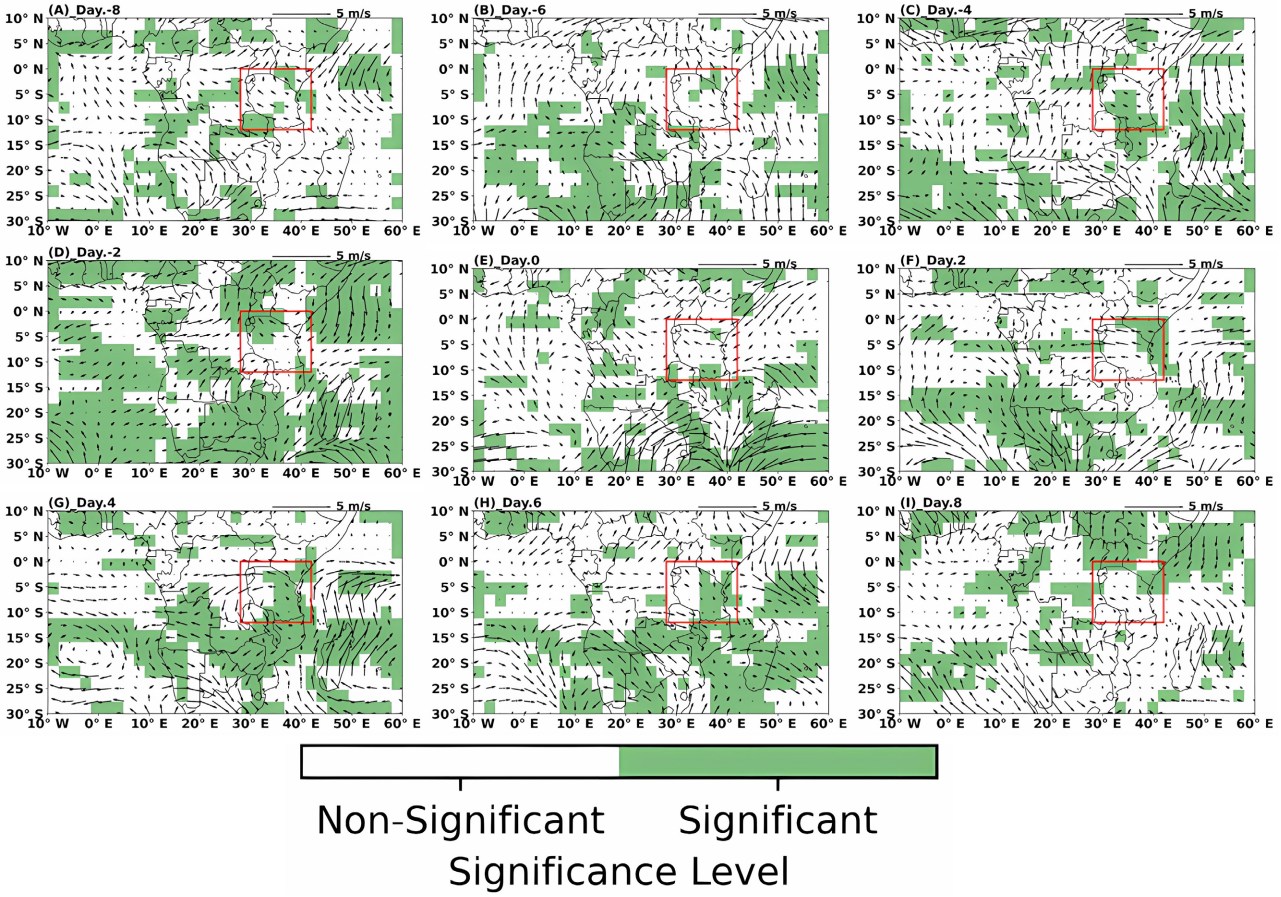

Figure 16. Composite maps of 850 hPa wind anomalies (vectors, units: m/s) filtered for 10 - 30-day oscillations during the MAM season of 2022, illustrating the quasi-biweekly rainfall variability over Tanzania. Panels (A) through (I) correspond to different lag days from Day −8 to Day +8, with Day 0 representing the peak rainfall phase. Significant areas are shaded in green, indicating regions where the wind anomalies are statistically significant, while non-significant regions are left unshaded. The red box highlights the study area over Tanzania, emphasizing the key spatial features of intraseasonal wind variability. Black vectors represent the direction and magnitude of the wind anomalies, with a reference scale of 3 m/s provided in the top right corner of each panel.

On Day −4 (Figure 17(C)), Tanzania and the surrounding regions show that divergence weakens but remains dominant. On Day −2 (Figure 17(D)), we recognize the emergence of convergence beginning to form over Tanzania, along with wind anomalies shifting inward toward the region, starting from 35˚E and 5˚S - 10˚S, indicating increasing upper-level moisture and potential for convective activity. The peak observed on Day 0 (Figure 17(E)) near Tanzania (30˚E - 40˚E, 5˚S - 5˚N) shows weak diverging wind patterns aloft that enhance upward motion and moisture from the low-level, creating favorable conditions for rainfall. After Day 0, divergence begins to rebuild on Day +2 (Figure 17(F)), indicating a return to the dry phase. Days +4 to +8 (Figures 17(G)-(I)) show a marked return to divergence over Tanzania and surrounding regions, especially around 30˚E - 40˚E and 5˚S - 10˚S, which is important for stabilizing drier conditions with reduced convective potential. This oscillating pattern of convergence and divergence, occurring approximately every 17 days, underlines the role of upper-level wind anomalies in modulating quasi-biweekly rainfall variability over Tanzania during

the MAM season.

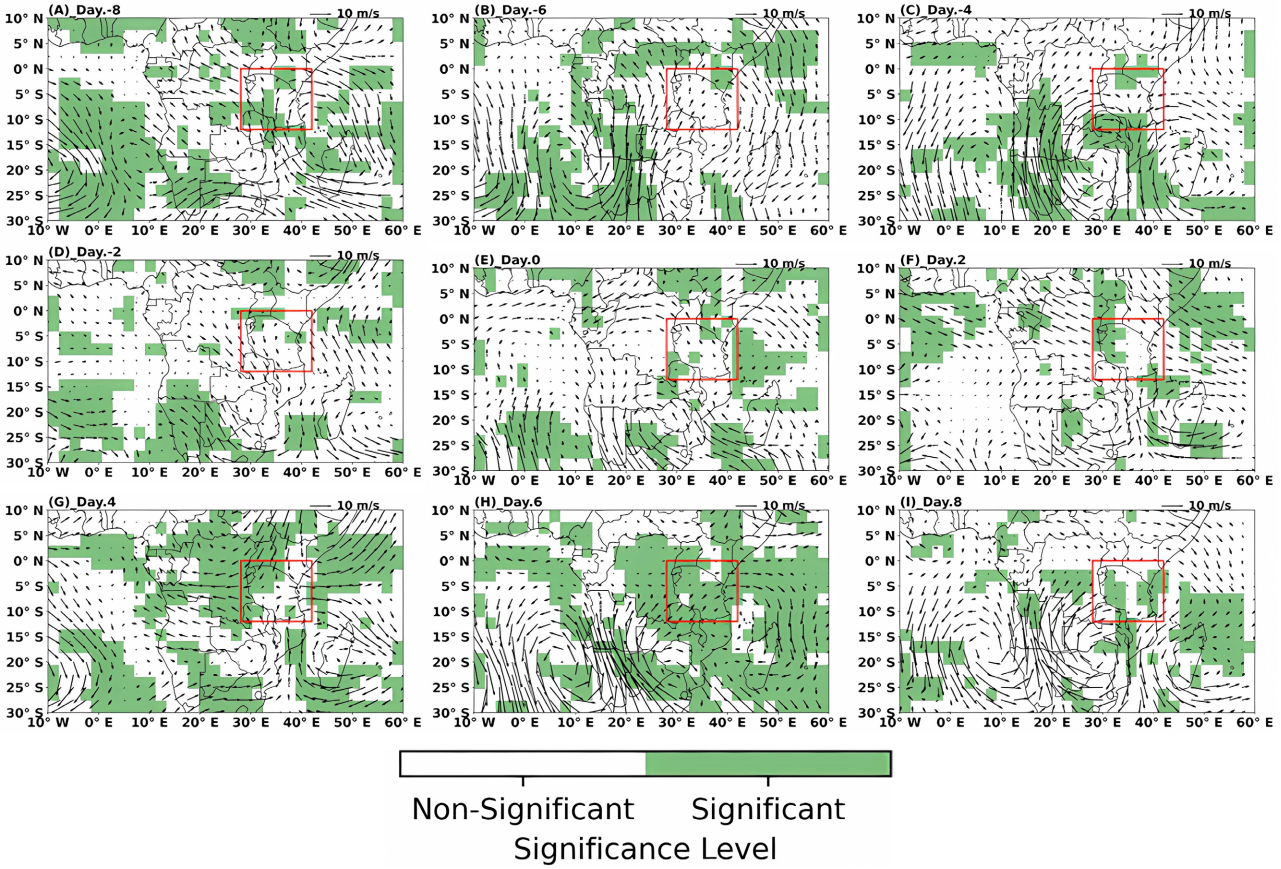

Figure 17. Composite maps of 200 hPa wind anomalies (vectors, units: m/s) filtered for 10 - 30-day oscillations during the MAM season of 2022, highlighting the quasi-biweekly rainfall variability over Tanzania. Panels (A) through (I) represent different lag days from Day −8 to Day +8, with Day 0 denoting the peak rainfall phase. Significant regions are shaded in green, while non-significant areas remain unshaded. The red box marks the study region over Tanzania, providing a focus on key spatial patterns of upper-level wind variability associated with intraseasonal rainfall oscillations. Black vectors depict wind anomaly magnitude and direction, with a reference scale of 10 m/s displayed in the top right corner of each panel.

5. Discussion and Conclusion

5.1. Discussion

The primary objective of this study was to investigate the ISV of rainfall during the MAM season of 2022. The dominant mode of intraseasonal variability (ISV) was analyzed using observational data from the Tanzania Meteorological Authority (TMA). The 5-day running mean during the MAM season reveals that Tanzania experienced an irregular pattern of wet and dry days in the year 2022, indicating the presence of ISV that leads to fluctuations in weather patterns. This fluactution of ISV has great impact in both social and economic welfare especially those living near major lakes, wetlands, and river flood valley. The high peak rainfall feed the land, filling lakes and rivers, which bring hope to fishermen and farmers as they plant seeds and expect good harvests. However, unpredictable ISV of rainfall can rapidly turn this expectation into fear, as changes in rainfall are often the

main reason for differences in crop yields. The effects of ISV of rainfall extend to fishing and livestock management as well, with insufficient rain causing fish populations to decline and pastures to dry up, forcing herders to travel long distances for animal feed. This implies that there should be better prediction of ISV of rainfall from the Meteorological Authorities for delivery of early warning and preparedness. Also the results showed the dominant peak date to be significant in the 10 - 25-day range, showing that ISV exhibits a quasi-biweekly. This finding aligns with previous research by [12], which identified a 10 - 20-day cycle using power spectrum analysis for the intraseasonal convective structure and evolution over tropical East Africa. Also, consistence with the studies of [15] [35] that examined the intraseasonal oscillation of rainfall variability. Further analysis from Fast Fourier Transform (FFT) showed quasi-biweekly pattern, lasting near 17 days, as shown in **Figure 5**. The results reveal three observed peaks, and composite analysis indicates the time evolution of rainfall in Tanzania during the MAM season ranges from −8 to +8 days, with day 0 representing the peak date. This understanding is crucial for Tanzania, since most of areas over the country are prone to floods and droughts. Knowing the quasi-biweekly oscillation is essential for weather-related departments to enhance early warning systems based on extended forecasts, and for disaster management teams to inform communities on how to prepare for flooding and droughts. Moreover, this study analyzed the influences of atmospheric circulation on intraseasonal variability (10 - 30 days) of rainfall over Tanzania during the MAM season of 2022. The results indicate that interactions between geopotential height anomalies and wind patterns at 850 hPa and 200 hPa has significant impact of ISV rainfall. At 850 hPa, negative geopotential height anomalies over the Western Indian Ocean and Mozambique Channel enhance low-level convergence of moisture, resulting in wet days while positive geopotential height anomalies are associated with divergence resulting in dry conditon. Strong positive geopotential height anomalies at 200 hPa are associated with upper-level divergence that supports peak rainfall (day 0). Also result from OLR indicated that Tanzania experienced significant positive OLR(OLR) anomalies of around 10 - 15 W/m^2, as seen in **Figure 12(A)** and **Figure 12(B)** at Lag −8 and Lag −6, indicating a decrease in cloud cover and convection. This led to dry condition, as moisture inflow from the Congo Basin, Mozambique Channel, and SWIO was minimum. At Lag 0 (**Figure 12(E)**), which corresponds to the peak date for rainfall, the results showed significant negative OLR values of around −18 W/m^2 to −20 W/m^2, and moisture convergence reached its highest point, resulting in a high rainfall. On other hand in **Figure 10** shows the region experiences dominant negative RH anomalies (−0.5% to −0.8%), characterized by weak low-level westerly winds initiating from the Congo Basin and northerly winds that take dry air into Tanzania, thus restricting moisture transport. On Day −4 (**Figure 10(C)**, these positive anomalies strengthen further as westerly winds enhance moisture transport from the Congo Basin, while easterly winds converge over Tanzania, leading to substantial moisture accumulation. This ends in the wettest phase

observed between Day −2 and Day 0 (**Figure 10(D)**, **Figure 10(E)**), when positive anomalies peak (0.8% to 1.0%) due to strong low-level convergence of westerly and easterly winds at 850 hPa, which lifts vertical motion and rainfall. These findings are consistent with previous studies, such as [9] [36]. In summary, the interplay between atmospheric circulation patterns and ISV of rainfall during the MAM season is complex, with significant implications for rainfall distribution, intensity, and overall climate variability in the region. Understanding these dynamics is essential for improving seasonal rainfall forecasts and managing water resources effectively. The findings underscore the importance of integrating ISV into weather forecasting and early warning systems to better prepare for and mitigate risks associated with extreme rainfall events, such as flooding or drought, in Tanzania and neighboring regions.

5.2. Conclusion

The main focus of the study was to investigate the intraseasonal variability of rainfall over Tanzania during the MAM season 2022. To support this objective, the analysis was conducted using various methods. A 5-day running average was employed on the observational data to smooth out fluctuations, while the power spectrum was utilized to identify the dominant modes of intraseasonal variability in rainfall during the MAM season over Tanzania. Furthermore, a composite method was applied to examine the atmospheric circulation influencing the intraseasonal variability of rainfall during the MAM season. The major findings are as follows: The 5-day running mean for the MAM season of 2022 shows that Tanzania undergoes an irregular pattern of wet and dry days, emphasizing the intraseasonal variability that leads to changes in weather patterns. This is illustrated by the early wet conditions in March, followed by a shift to drier conditions beginning in mid-April, as indicated by the running mean falling below zero. Power spectrum analysis and Fast Fourier Transform (FFT) results indicate that Tanzania's rainfall during the MAM season is significantly influenced by intraseasonal variability. This variability is characterized by a dominant quasi-biweekly pattern, with a peak in the 10 - 25-day range, particularly around 17 days. The composite analysis of atmospheric circulation during the March-April-May (MAM) season provides key insights into the ISV of rainfall over Tanzania and points out how they affect intraseasonal variability (ISV). The findings suggest that the interactions between geopotential height anomalies and wind patterns at 850 hPa and 200 hPa significantly influence ISV rainfall. At 850 hPa, negative geopotential height anomalies over the Western Indian Ocean and the Mozambique Channel promote low-level moisture convergence, leading to wet days, whereas positive geopotential height anomalies are linked to divergence, causing dry conditions. Additionally, strong positive geopotential height anomalies at 200 hPa are related to the upper-level divergence that facilitates peak rainfall (day 0). Further investigation reveals that the peak ISV of rainfall at Lag 0 at 850 hPa was characterized by positive RH anomalies of moisture transport from the SWIO, Congo Basin, and Mozambique

Channel towards the region, while After Lag 0, moisture contributions from these regions reduced, leading to a shift toward drier conditions (lag −8). Over Tanzania during Lag −4 to Lag 0, results revealing a negative OLR anomaly (−18 to −20 m/w^2) dominate that indicating peak ISV of rainfall supported by the SWIO and the Congo Basin. The evolution to positive OLR anomalies after Lag +2 shows the starting point of a dry phase of ISV. Furthermore, at the initial phase (Lag −8 to Lag −6), weak positive anomalies and limited moisture flux were observed over Tanzania, while in the peak phase (Lag 0), strong positive anomalies dominated Tanzania, reflecting intense moisture convergence from both the SWIO and the Congo Basin, associated with maximum ISV of rainfall activity. From lag 0, transition into the dry phase (Lag +6 to Lag +8), negative anomalies develop as moisture transport diminishes and winds shift, suppressing convergence over Tanzania, and leading to reduced rainfall. Generally, ISV of rainfall in Tanzania during the MAM season has significant implications for both fisheries and farmers, affecting water availability, crop yields, and environmental stability positively or negatively. It was noted that the irregular timing of dry and wet periods leads to droughts or floods, which strictly impact crop production and threaten food security, especially for smallholder farmers who are dependent on rain-fed agriculture. Also, it was found that ISV in rainfall disrupts marine ecosystems, affecting fish populations and altering water quality in coastal areas. The results also show that both farmers and fishers face sharp ISV of rainfall due to climate change, which leads to economic instability and increased migration to urban areas in search of better opportunities. Further studies should focus on developing and evaluating statistical and dynamical models for predicting ISV of rainfall during the MAM season in Tanzania. In this regard, the Meteorological department in Tanzania must improve early warning systems and the Government should provide capacity building for farmers by providing training and resources on adaptive strategies for managing the impacts of ISV, including crop rotation and diversification.

Acknowledgements

The first author is appreciative to acknowledge the Climate Hazards Group Infrared Precipitation with Station (CHIRPS) for making the data available and Atmospheric data from NOAA, Tanzania Meteorological Authority and the Ministry of Commerce of China (MOFCOM) for providing opportunity to carry on with studies. Much thanks to Prof. Shuangyan Yang for supervision as well as providing guidance on this research.

Conflicts of Interest

The authors declare that there is no conflict of interest regarding the publication of this paper.

References

[1] Wani, S.P., Sreedevi, T.K., Rockström, J. and Ramakrishna, Y.S. (2009) Rainfed

Agriculture—Past Trends and Future Prospects. In: Wani, S.P., Rockström, J. and Oweis, T., Eds., *Rainfed Agriculture*: *Unlocking the Potential*, CABI, 1-35. https://doi.org/10.1079/9781845933890.0001

[2] Mafuru, K.B. and Guirong, T. (2018) Assessing Prone Areas to Heavy Rainfall and the Impaction of the Upper Warm Temperature Anomaly during March-May Rainfall Season in Tanzania. *Advances in Meteorology*, **2018**, Article ID: 8353296. https://doi.org/10.1155/2018/8353296

[3] TMA (2022) Statement on the Status of Tanzania Climate in 2022. No. 1130, p. 21. https://www.meteo.go.tz/uploads/publications/en1680520682-Tanzania%20Climate%20Statetement%202022.pdf

[4] United Nations Office for the Coordination of Humanitarian Affairs (2023) Tanzania: Heavy Rains and Flooding Flash Update No. 2, 12 December 2023. https://www.unocha.org/publications/report/united-republic-tanzania/tanzania-heavy-rains-and-flooding-flash-update-no-2-12-december-2023

[5] Mapande, A.T. and Reason, C.J.C. (2005) Interannual Rainfall Variability over Western Tanzania. *International Journal of Climatology*, **25**, 1355-1368. https://doi.org/10.1002/joc.1193

[6] Saji, N.H., Goswami, B.N., Vinayachandran, P.N. and Yamagata, T. (1999) A Dipole Mode in the Tropical Indian Ocean. *Nature*, **401**, 360-363. https://doi.org/10.1038/43854

[7] Kiladis, G.N., Wheeler, M.C., Haertel, P.T., Straub, K.H. and Roundy, P.E. (2009) Convectively Coupled Equatorial Waves. *Reviews of Geophysics*, **47**, RG2003. https://doi.org/10.1029/2008rg000266

[8] Waiswa, M. (2015) Assessment of Spatial and Temporal Characteristics of the December-February Seasonal Rains over Uganda Milton. https://api.semanticscholar.org/CorpusID:55662790

[9] Nicholson, S.E. (2017) Climate and Climatic Variability of Rainfall over Eastern Africa. *Reviews of Geophysics*, **55**, 590-635. https://doi.org/10.1002/2016rg000544

[10] Anyah, R.O., Semazzi, F.H.M. and Xie, L. (2006) Simulated Physical Mechanisms Associated with Climate Variability over Lake Victoria Basin in East Africa. *Monthly Weather Review*, **134**, 3588-3609. https://doi.org/10.1175/mwr3266.1

[11] Madden, R.A. and Julian, P.R. (1971) Detection of a 40-50 Day Oscillation in the Zonal Wind in the Tropical Pacific. *Journal of the Atmospheric Sciences*, **28**, 702-708. https://doi.org/10.1175/1520-0469(1971)028<0702:doadoi>2.0.co;2

[12] Mpeta, E. and Jury, M. (2001) Intra-seasonal Convective Structure and Evolution over Tropical East Africa. *Climate Research*, **17**, 83-92. https://doi.org/10.3354/cr017083

[13] Kabanda, T. and Jury, M. (2000) Synoptic Evolution of Composite Wet Spells over Northern Tanzania. *Climate Research*, **15**, 239-248. https://doi.org/10.3354/cr015239

[14] Krishnamurthy, V. and Shukla, J. (2007) Intraseasonal and Seasonally Persisting Patterns of Indian Monsoon Rainfall. *Journal of Climate*, **20**, 3-20. https://doi.org/10.1175/jcli3981.1

[15] Zhou, X., Chen, L., Umuhoza, J., Cheng, Y., Wang, L. and Wang, R. (2021) Intraseasonal Oscillation of the Rainfall Variability over Rwanda and Evaluation of Its Subseasonal Forecasting Skill. *Atmospheric and Oceanic Science Letters*, **14**, Article ID: 100099. https://doi.org/10.1016/j.aosl.2021.100099

[16] Wamba Tchinda, C., Tchakoutio Sandjon, A., Djiotang Tchotchou, A.L., Nzeudeu Siwe, A., Vondou, D.A. and Nzeukou, A. (2023) The Influence of Intraseasonal

Oscillations on Rainfall Variability over Central Africa: Case of the 25-70 Days Variability. *Scientific Reports*, **13**, Article No. 19842.
https://doi.org/10.1038/s41598-023-46346-y

[17] Kebacho, L.L. (2022) Interannual Variations of the Monthly Rainfall Anomalies over Tanzania from March to May and Their Associated Atmospheric Circulations Anomalies. *Natural Hazards*, **112**, 163-186.
https://doi.org/10.1007/s11069-021-05176-9

[18] Makula, E.K. and Zhou, B. (2021) Changes in March to May Rainfall over Tanzania during 1978-2017. *International Journal of Climatology*, **41**, 5663-5675.
https://doi.org/10.1002/joc.7146

[19] King'uza, P. and Tilwebwa, S. (2019) Inter-Annual Variability of March to May Rainfall over Tanzania and Its Association with Atmospheric Circulation Anomalies. *Geographica Pannonica*, **23**, 147-161. https://doi.org/10.5937/gp23-22430

[20] International Monetary Fund (2022) United Republic of Tanzania. IMF Staff Country Reports, 1. https://doi.org/10.5089/9798400215414.002

[21] Kazora, J., Zhu, W., Kyaw, T.O., Sebaziga, J.N., Rusanganwa, F. and Kagabo, J. (2023) Enhancement of East African Monsoon Long Rainfall (March to May) Variability from Weekly to Annual Scale by Climatic Extremes. *Atmospheric and Climate Sciences*, **13**, 491-506. https://doi.org/10.4236/acs.2023.134028

[22] Roy, I. and Troccoli, A. (2024) Identifying Important Drivers of East African October to December Rainfall Season. *Science of the Total Environment*, **914**, Article ID: 169615. https://doi.org/10.1016/j.scitotenv.2023.169615

[23] Kijazi, A.L. and Reason, C.J.C. (2005) Relationships between Intraseasonal Rainfall Variability of Coastal Tanzania and Enso. *Theoretical and Applied Climatology*, **82**, 153-176. https://doi.org/10.1007/s00704-005-0129-0

[24] Vashisht, A. and Zaitchik, B. (2022) Modulation of East African Boreal Fall Rainfall: Combined Effects of the Madden-Julian Oscillation (MJO) and El Niño-Southern Oscillation (ENSO). *Journal of Climate*, **35**, 2019-2034.
https://doi.org/10.1175/jcli-d-21-0583.1

[25] Kai, K.H., Ngwali, M.K. and Faki, M.M. (2021) Assessment of the Impacts of Tropical Cyclone Fantala to Tanzania Coastal Line: Case Study of Zanzibar. *Atmospheric and Climate Sciences*, **11**, 245-266. https://doi.org/10.4236/acs.2021.112015

[26] Hu, Y., Li, D. and Liu, J. (2007) Abrupt Seasonal Variation of the ITCZ and the Hadley Circulation. *Geophysical Research Letters*, **34**.
https://doi.org/10.1029/2007gl030950

[27] Dinku, T., Funk, C., Peterson, P., Maidment, R., Tadesse, T., Gadain, H., *et al.* (2018) Validation of the CHIRPS Satellite Rainfall Estimates over Eastern Africa. *Quarterly Journal of the Royal Meteorological Society*, **144**, 292-312.
https://doi.org/10.1002/qj.3244

[28] Kanamitsu, M., *et al.* (2002) Ncep-Doe AMIP-II Reanalysis (R-2).
https://doi.org/10.1175/BAMS-83-11-1631

[29] Pan, W., Mao, J. and Wu, G. (2013) Characteristics and Mechanism of the 10-20-Day Oscillation of Spring Rainfall over Southern China. *Journal of Climate*, **26**, 5072-5087. https://doi.org/10.1175/jcli-d-12-00618.1

[30] Kikuchi, K., Wang, B. and Kajikawa, Y. (2011) Bimodal Representation of the Tropical Intraseasonal Oscillation. *Climate Dynamics*, **38**, 1989-2000.
https://doi.org/10.1007/s00382-011-1159-1

[31] Wilks, D.S. (2007) Statistical Methods in the Atmospheric Sciences. Vol. 91, 2nd

Edition, Academic Press.

[32] Roberts, J.L. (1978) Ram Gill Ventilation in Fish. In: Sharp, G.D. and Dizon, A.E., Eds., *The Physiological Ecology of Tunas*, Elsevier, 83-88. https://doi.org/10.1016/b978-0-12-639180-0.50012-4

[33] Huang, Q., Yin, X. and Yao, S. (2021) The Quasi-Biweekly Oscillation of Summer Rainfall in Southern China and Its Relationship with the Geopotential Height Anomaly over the North Atlantic Ocean. *Frontiers in Earth Science*, **9**, Article ID: 770253. https://doi.org/10.3389/feart.2021.770253

[34] Clark, C.O., Webster, P.J. and Cole, J.E. (2003) Interdecadal Variability of the Relationship between the Indian Ocean Zonal Mode and East African Coastal Rainfall Anomalies. *Journal of Climate*, **16**, 548-554. https://doi.org/10.1175/1520-0442(2003)016<0548:ivotrb>2.0.co;2

[35] Sandjon, A.T., Nzeukou, A. and Tchawoua, C. (2012) Intraseasonal Atmospheric Variability and Its Interannual Modulation in Central Africa. *Meteorology and Atmospheric Physics*, **117**, 167-179. https://doi.org/10.1007/s00703-012-0196-6

[36] Koster, R.D., Walker, G.K., Mahanama, S.P.P. and Reichle, R.H. (2014) Soil Moisture Initialization Error and Subgrid Variability of Precipitation in Seasonal Streamflow Forecasting. *Journal of Hydrometeorology*, **15**, 69-88. https://doi.org/10.1175/jhm-d-13-050.1